2015-03

# Using potential vorticity to characterize the forcing of a coastally trapped wind reversal along the California coast

Morris, Christopher M.

Monterey, California: Naval Postgraduate School


# NAVAL POSTGRADUATE SCHOOL

**MONTEREY, CALIFORNIA**

# THESIS

**USING POTENTIAL VORTICITY TO CHARACTERIZE THE FORCING OF A COASTALLY TRAPPED WIND REVERSAL ALONG THE CALIFORNIA COAST**

by

Christopher M. Morris

March 2015

Thesis Advisor: Wendell Nuss
Second Reader: Qing Wang

**Approved for public release; distribution is unlimited**

THIS PAGE INTENTIONALLY LEFT BLANK

# REPORT DOCUMENTATION PAGE

*Form Approved OMB No. 0704–0188*



| 1. AGENCY USE ONLY *(Leave blank)* | 2. REPORT DATE | 3. REPORT TYPE AND DATES COVERED |
|---|---|---|
| | March 2015 | Master's Thesis |

**4. TITLE AND SUBTITLE**
USING POTENTIAL VORTICITY TO CHARACTERIZE THE FORCING OF A COASTALLY TRAPPED WIND REVERSAL ALONG THE CALIFORNIA COAST

**5. FUNDING NUMBERS**

**6. AUTHOR(S)** Christopher M. Morris

**7. PERFORMING ORGANIZATION NAME(S) AND ADDRESS(ES)**
Naval Postgraduate School
Monterey, CA 93943-5000

**8. PERFORMING ORGANIZATION REPORT NUMBER**

**9. SPONSORING /MONITORING AGENCY NAME(S) AND ADDRESS(ES)**
N/A

**10. SPONSORING/MONITORING AGENCY REPORT NUMBER**

**11. SUPPLEMENTARY NOTES** The views expressed in this thesis are those of the author and do not reflect the official policy or position of the Department of Defense or the U.S. Government. IRB Protocol number ____N/A____.

**12a. DISTRIBUTION / AVAILABILITY STATEMENT**
Approved for public release; distribution is unlimited

**12b. DISTRIBUTION CODE**

**13. ABSTRACT (maximum 200 words)**

Using the Climate Forecast System Reanalysis (CFSR) dataset, the synoptic environment of six historical coastally trapped wind reversals (CTWR) along the California coast is examined. Building on the Mass and Bond climatology of 1996, the study uses potential vorticity (PV) as a proxy for the coastal jet and seeks to characterize the forcing of the CTWRs by analyzing their 950-mb potential vorticity plumes. The study also pursues the ability to separate geostrophically-balanced wind reversals synonymous with synoptic systems from unbalanced wind reversals (CTWRs) by taking advantage of the invertibility of PV and using the inversion technique outlined in the August 1991 issue of *Monthly Weather Review* by Christopher Davis and Kerry Emanuel. The study then applied the methodology to data from July/August 2012/2013 in order to uncover possible CTWRs. The primary findings of this study are as follows: 1) the potential vorticity maximum generated through the offshore flow of the coastal jet is required to move off shore and establish an across-coast PV gradient in order for a CTWR to form/propagate northward of Point Conception and 2) the Davis Emanuel PV inversion technique yielded mixed results, heavily influenced by diurnal effects and subjected to instability due to topographical interactions.

| 14. SUBJECT TERMS | 15. NUMBER OF PAGES |
|---|---|
| coastally trapped wind reversal, potential vorticity, PV inversion, coastal meteorology | 81 |
| | 16. PRICE CODE |

| 17. SECURITY CLASSIFICATION OF REPORT | 18. SECURITY CLASSIFICATION OF THIS PAGE | 19. SECURITY CLASSIFICATION OF ABSTRACT | 20. LIMITATION OF ABSTRACT |
|---|---|---|---|
| Unclassified | Unclassified | Unclassified | UU |

NSN 7540–01-280-5500

Standard Form 298 (Rev. 2–89)
Prescribed by ANSI Std. 239–18

THIS PAGE INTENTIONALLY LEFT BLANK

**Approved for public release; distribution is unlimited**

# USING POTENTIAL VORTICITY TO CHARACTERIZE THE FORCING OF A COASTALLY TRAPPED WIND REVERSAL ALONG THE CALIFORNIA COAST

Christopher M. Morris
Lieutenant Commander, United States Navy
B.S., United States Air Force Academy, 2004
B.S., Naval Postgraduate School, 2005
M.A., Liberty University, 2008

Submitted in partial fulfillment of the
requirements for the degree of

**MASTER OF SCIENCE IN METEOROLOGY AND PHYSICAL OCEANOGRAPHY**

from the

**NAVAL POSTGRADUATE SCHOOL**
**March 2015**

Author: Christopher M. Morris

Approved by: Wendell Nuss
Thesis Advisor

Qing Wang
Second Reader

Wendell Nuss
Chair, Department of Meteorology

THIS PAGE INTENTIONALLY LEFT BLANK

# ABSTRACT

Using the Climate Forecast System Reanalysis (CFSR) dataset, the synoptic environment of six historical coastally trapped wind reversals (CTWR) along the California coast is examined. Building on the Mass and Bond climatology of 1996, the study uses potential vorticity (PV) as a proxy for the coastal jet and seeks to characterize the forcing of the CTWRs by analyzing their 950-mb potential vorticity plumes. The study also pursues the ability to separate geostrophically-balanced wind reversals synonymous with synoptic systems from unbalanced wind reversals (CTWRs) by taking advantage of the invertibility of PV and using the inversion technique outlined in the August 1991 issue of *Monthly Weather Review* by Christopher Davis and Kerry Emanuel. The study then applied the methodology to data from July/August 2012/2013 in order to uncover possible CTWRs. The primary findings of this study are as follows: 1) the potential vorticity maximum generated through the offshore flow of the coastal jet is required to move off shore and establish an across-coast PV gradient in order for a CTWR to form/propagate northward of Point Conception and 2) the Davis Emanuel PV inversion technique yielded mixed results, heavily influenced by diurnal effects and subjected to instability due to topographical interactions.

THIS PAGE INTENTIONALLY LEFT BLANK

# TABLE OF CONTENTS

THIS PAGE INTENTIONALLY LEFT BLANK

# LIST OF FIGURES

THIS PAGE INTENTIONALLY LEFT BLANK

# LIST OF TABLES

THIS PAGE INTENTIONALLY LEFT BLANK

# ACKNOWLEDGMENTS

I would like to thank CDR Bill Sommer for his flexibility and out-of-the-box thinking as my program officer and for his timely and much-needed assistance with teaching Sunday School at our church. I am also in great debt to Professor Wendell Nuss, without whom I would not have come close to completing the task of graduating from the Naval Postgraduate School. Finally, there is a special place in my heart for my incredibly beautiful and understanding wife, Stephanie, who never doubted (for too long anyways) and always enabled me to put my best foot forward—thank you; I love you!

THIS PAGE INTENTIONALLY LEFT BLANK

# I. INTRODUCTION

During the warm summer season, California's coastal climate is predominately characterized by northerly winds stemming from a subtropical anticyclone, the eastern Pacific High located about 1000 kilometers offshore (Dorman 1987). In addition to transporting subsiding air to warm the atmosphere aloft, the eastern Pacific High creates cooler temperatures at the surface as the northerly winds enable coastal upwelling through Ekman processes. Thus, the West Coast of the United States is characterized by a Marine Boundary Layer (MBL) bounded to its east by coastal topography reaching over 500 meters and aloft by a temperature inversion on the order of 10-degrees Celsius (Dorman 1987).

Approximately twice a month, the northerly winds are disrupted by relatively short, 1- to 3-day periods of southerly winds (Bond et al. 1996). Often characterized as a "stratus surge" (Felsch and Whitlatch 1993) or "southerly surge," we will take the lead from Nuss et al. (2000) and refer to these disturbances as a coastally trapped wind reversal (CTWR). A plethora of work has been done to explain the dynamics behind the southerly winds. Dorman (1985) presented a case for a Kelvin wave and for a gravity current (Dorman 1987), while Mass and Albright (1987) suggested that the southerly winds were caused by an ageostrophic response to a synoptically-driven change in the alongshore pressure gradient. Additionally, Nuss (2007) concluded that the reversal, regardless of the dynamics behind it, sometimes propagates northward or sometimes does not propagate at all.

Wind reversals are typically characterized by an abrupt change in the winds and the northward movement of narrow bands of stratus. As such, CTWRs present a challenging forecast problem and can place naval operations at risk. Due to the rapid timescale on which the weather conditions can change, CTWRs can make navigation unsafe for mariners and lead to placing unprepared aviators at risk of flying under unexpectedly adverse weather conditions. Mass and Albright (1987) found that in some cases the winds could shift from moderate northerlies (0-10 $ms^{-1}$) to southerlies of 15 $ms^{-1}$ or more, temperatures could fall in excess of 10-degrees Celsius and clear skies

could be overtaken by severe fog—all in less than an hour. These changes are often not captured by models and require a keen forecast for proper preparation. Consequently, the ability to fully understand and accurately predict these wind reversals remains critical.

# II. BACKGROUND

## A. DEFINITION AND CLIMATOLOGY OF A CTWR

In simplest terms, a coastally trapped wind reversal (CTWR) is a disruption of the climatological flow due to a mesoscale phenomenon. It usually has a length of about 1000 kilometers in the alongshore direction and an across-shore width of approximately 100–300 kilometers (Reason and Steyn 1990). Furthermore, CTWRs generally replace dry, clear sky conditions with low-level stratus or fog (Reason and Steyn 1990). Reason and Steyn (1990) point out four global regions in which the interaction of mid-latitude weather and coastal topography provides the necessary ingredients for the generation of a CTWR (see Figure 1). This paper will focus on CTWRs occurring off the west coast of California, of which there are approximately two per month lasting an average of 30 hours each (Bond et al. 1996).

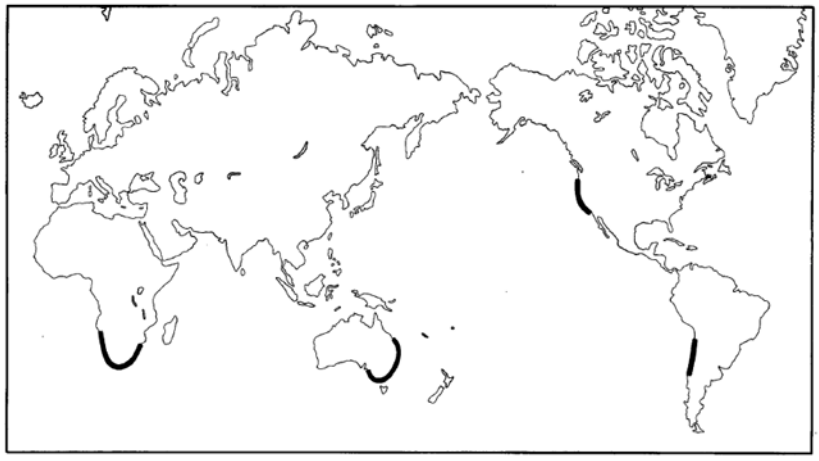

Figure 1. World map showing CTWR-favorable regions in bold (from Reason and Steyn 1990).

Bond et al. (1996) provides a definitive climatology of the characteristics of a CTWR along the west coast of the United States. In compiling their extensive climatology, they looked at data from four buoy stations during the warm season (April-September) over a period of 10 years (1981–1991) and utilized specific criteria that we

will adopt as our definition of a CTWR. Understanding that a CTWR will typically show up as an abrupt shift (reversal) of the winds, they declared the onset of a reversal as the first hour of sustained southerly wind. Additionally, they required the winds to have had a northerly component for at least 11 of the 12 hours preceding the onset of southerly winds. Finally, Bond et al. (1996) required that southerlies be observed for 10 of the next 12 hours (southerlies defined as winds within 45 degrees of the orientation of the coastline).

It is important to note that Bond et al. (1996) used a subjective analysis to reject as CTWRs any reversal of the winds that were the geostrophically-balanced result of a low-pressure system or land-falling synoptic system (frontal passage). Their aim was to capture southerly flow that was often highly ageostrophic and restricted to within approximately one Rossby radius of the coastal topography, where topographic blocking by the terrain would play a contributing role. Bond et al. (1996) further classified CTWRs as either "strong" or "weak" disturbances. To qualify as a strong event, there must have been at least one hour with a southerly component greater than or equal to 5 $ms^{-1}$.

Mass and Bond (1996) examined the same ten years' worth of reversals discussed in the previous paragraph and described the typical synoptic evolution associated with a CTWR. In order to arrive at their generalized description, Mass and Bond (1996) started by creating the climatological (1964–1989) analysis for five parameters: sea level pressure (SLP), 850-mb geopotential height, 850-mb wind, 850-mb temperature, and 500-mb geopotential height (see Figure 2). After establishing a baseline, Mass and Bond (1996) once again separated the strong reversals from the weak ones. For each type of reversal, they focused on one of the four coastal buoys at a time during the onset of the CTWR and created a set of composite analyses (each set containing each of the five parameters). With the completion of both the climatology and the analysis, Mass and Bond then drew general conclusions about the deviations from climatology during a CTWR at each buoy.

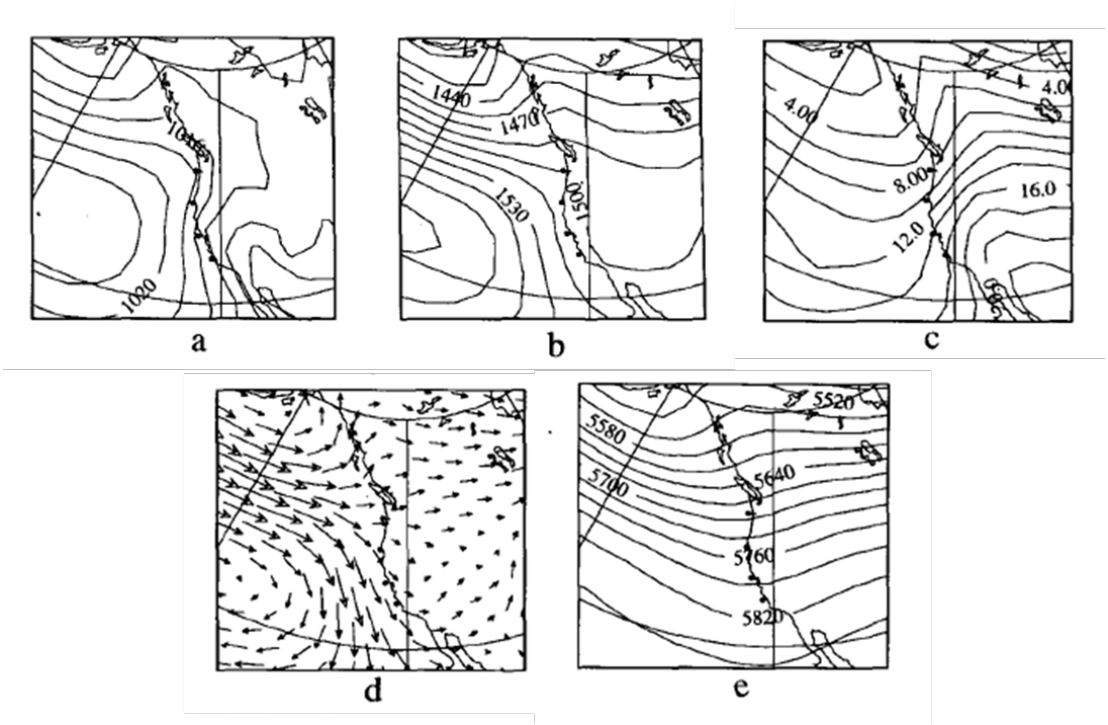


Figure 2. Warm season (April-September) (a) climatology of SLP, (b) 850-mb geopotential heights, (c) 850-mb temperature, (d) 850-mb winds, (e) and 500-mb heights. Heights are in meters, temperatures are in degrees Celsius, and the maximum 850-mb wind vector is 9.7 $ms^{-1}$. The black dots indicate the four buoy locations (from Mass and Bond 1996).

Mass and Bond (1996) discovered that the synoptic evolution at each of the four buoys (ranging from southern California to the Columbia River) was very similar in the day or two prior to the onset of a CTWR:

- An anomalous ridge at 500 mb pushes eastward into the Pacific Northwest while an upper-level trough tilts to the northeast as its northern portion is advected eastward and its southern part remains anchored over California.
- 850-mb ridging over the eastern Pacific amplifies and also pushes into the Pacific Northwest while weak troughing extends westward over coastal California.
- Surface northerlies increase in amplitude as the eastern Pacific High strengthens and pushes into the Pacific Northwest. Furthermore, thermal troughing situated in the central valleys of California pushes westward into the coastal region.

Due to the factors just listed, the composite sea level pressure patterns accompanying CTWRs at all four buoys are associated with an anomalous alongshore

pressure gradient: instead of the usual equatorward decrease of pressure along the Californian coast, pressure either increases or remains approximately constant in the composites to the south of the buoys during periods of trapped southerly flow (Mass and Bond 1996).

Despite the thoroughness of this climatology, recent data may be able to provide additional information beyond the reach of the 383-km resolution dataset utilized by Mass and Bond (1996). The Climate Forecast System Reanalysis (CFSR) data used in this thesis has a resolution that is approximately an order of magnitude smaller (50 km). Accordingly, we hope to add additional insight regarding the synoptic environment that surrounds a CTWR.

## B. CTWR DYNAMICS AND ESSENTIAL ENVIRONMENTAL FEATURES

A wave of studies from the mid-1980s through the 1990s shed light on the dynamics driving a CTWR. While some authors used individual case studies to draw a universal conclusion (Mass and Albright 1987), others attempted to explain the phenomenon through a variety of dynamical mechanisms (Dorman 1985; Dorman 1987). Parish et al. (2008) provides a thorough overview on the different discussions regarding CTWRs.

### 1. CTWR Dynamics

CTWRs are often interpreted as a Kelvin wave. A Kelvin wave is characterized by its northward propagation, little to no temperature change across the wind reversal, and a difference in wind speed and propagation speed. Additionally, a CTWR classified as a Kelvin wave can often be identified in satellite imagery by a steady northward progression of coastal stratus or fog (see Figure 3). Dorman (1985) first presented the case that a CTWR is an internal solitary Kelvin wave existing in the marine layer. Through an in-depth case study of a CTWR from June 1994 (Ralph et al. 1998), a subsequent paper by Ralph et al. (2000) suggests that CTWRs are best characterized as a hybrid of motions referred to as a mixed Kelvin wave bore (Parish et al. 1998).

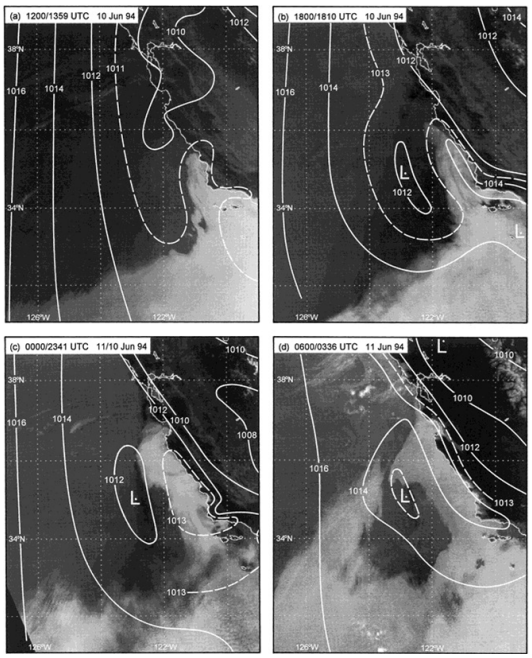


Figure 3. Sequence of visible satellite images from a NOAA polar-orbiting satellite at 1359, 1810, and 2341 UTC 10 June 1994, and infrared image from the same satellite at 0336 UTC 11 June. Mesoscale sea level pressure (mb) analyses are superimposed on each image. The time of each pressure analysis is shown followed by the time of each image (from Ralph et al. 1998).

Another interpretation of a CTWR is that of a topographically trapped density current, or gravity current. Dorman (1987) proposed this mechanism to explain why some CTWRs did not seem to propagate steadily northward along the California coast. A gravity current is triggered when onshore flow pools mass against the coastal mountains while the strong inversion prevents the increased MBL from escaping eastward over the mountains. Instead, the increased MBL leads to higher pressure to the south and a reversal of the winds. Gravity currents can be characterized by the similarity between their southerly wind strength and propagation speed, cooler temperatures on the south side of the wind shift, blocking and surges (Dorman 1987) and the absence of a "rising" and "falling" MBL. Rather, the marine layer is lifted and remains lifted (Dorman 1987).

A third proposed dynamics behind a CTWR is that the southerly flow is a direct response by the marine layer to an alongshore synoptic-scale pressure gradient (Mass and Albright 1987). Whereas the dynamics governing a Kelvin wave or gravity current rely

on the synoptic situation to create a favorable MBL, Mass and Albright's (1987) hypothesis regarding a CTWR as an ageostrophic response to the synoptic pattern is more dependent on the synoptic environment to act as a modulating force on the along-shore pressure gradient. Regardless of the dynamics one chooses to characterize a CTWR, an anomalous (high pressure to the south with lower pressure to the north) alongshore pressure gradient is required (Mass and Bond 1996; Mass and Albright 1987).

There is no doubt that understanding the dynamics behind a particular reversal is important in forecasting its associated weather. For example, Nuss (2007) found that CTWRs driven by Kelvin waves were more likely to propagate northward and carry with it the weather illustrated in Figure 3 whereas CTWRs driven by a gravity current tended to not progress steadily northward (Dorman 1987; Nuss 2007). What is less clear is the link between the synoptic environment identified by Mass and Bond (1996) and the dynamics driving a CTWR. Because of the coarse resolution of their dataset (~383 km), Mass and Bond (1996) were only able to offer a broad characterization of the synoptic environment required to facilitate a CTWR. They were unable to highlight synoptic subtleties that may have contributed to the different types of CTWRs discussed here. Nuss (2007) pointed out such differences in the Mass and Bond (1996) climatology that may have decided when a certain CTWR propagates or not. This thesis will focus on the synoptic environment enabling a CTWR by building on the Mass and Bond (1996) climatology through the analyses of potential vorticity using the CFSR dataset.

## 2. Coastal Jet

Under the influence of the semi-permanent eastern Pacific high-pressure system, which usually dictates the prevailing winds along the California coast during the warmer summer months, winds off the California coast typically blow from the north-northwest. As the northerly winds produce surface stress on the upper layers of the ocean, balance between the stress and the Coriolis force enables strong upwelling due to Ekman transport. This upwelling brings colder waters to the ocean's surface, cooling the lower layer of the atmosphere in the process. Coupled with the subsidence from the eastern Pacific High, the cooler lower atmosphere is subjected to a strong temperature inversion

on the order of 10-degrees Celsius (Dorman 1987) that, with aid of coastal terrain that extends to well over 1000 meters (see Figure 4), keeps the MBL in place. The formation of the temperature inversion and strong across-coast temperature gradient enables the development of a formidable coastal jet. It is our contention that the coastal jet is a key contributor to making the synoptic environment viable for the release of a CTWR as the coastal jet plays a vital role in the development of potential vorticity (PV).

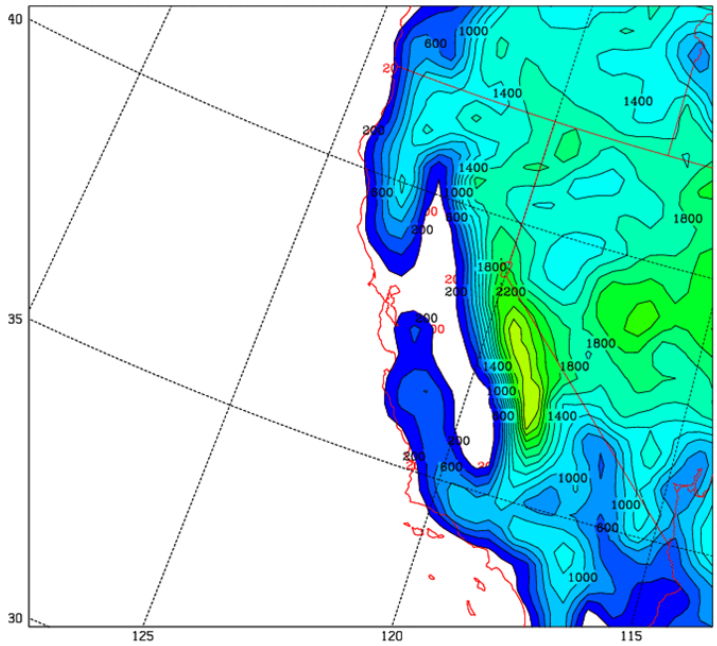


Figure 4. Topography of California created from the CFSR dataset. Elevations start at sea level (white) and increase at 200-m intervals.

### 3. Generation of Potential Vorticity

PV is a conserved quantity that is the product of absolute vorticity and static stability. Persson (1995) demonstrated that PV can be generated off the coast of northern California when the synoptic features, discussed by Mass and Bond (1996), set up offshore flow and combine with the MBL-features that strengthen the coastal jet. Persson (1995) and Skamarock (1998) both demonstrated that when the offshore flow interacts with the coastal mountains, horizontal shear is introduced as friction from the mountains causes a horizontal gradient in the winds. The across-coast wind gradient subsequently results in the development of PV. Development of the PV plume is only further

encouraged as the strong temperature inversion above the MBL entices the development of a low-level coastal jet and even stronger northerlies. The stronger the northerlies, the more potential for the development of a PV plume with greater amplitude.

A characteristic of PV that makes it appealing for use in this study is that it induces a circulation in much the same way as a low- or high-pressure system. Positive PV anomalies lead to a cyclonic circulation whereas as negative PV anomalies prompt an anti-cyclonic circulation. Furthermore, since PV is a conserved quantity in the absence of heat and friction (in our case, as the PV plume separates from the coast and the associated topography) the dynamically-balanced flow can be obtained through the process of invertibility (Davis and Emanuel 1991). Additionally, because of the mesoscale-nature of a CTWR, global models theoretically do not have sufficient resolution to resolve the highly unbalanced southerly winds of a CTWR. Accordingly, there must be a larger-scale feature reflected in the global models that is capable of relaying mesoscale information. One possible parameter is the potential vorticity conserved in the absence of diabatic heating and friction.

## C. THESIS OBJECTIVES

High-resolution global models have the resolution to show the evolution of potential vorticity, in this case the evolution of PV created through offshore flow as the flow interacts with complex topography in the vicinity of northern California (Persson 1995). Therefore, PV plumes generated off the California coast can serve as an excellent lens through which to characterize the forcing of a CTWR.

This paper will focus on using potential vorticity to both characterize the synoptic environment required to force a CTWR and to separate balanced from unbalanced flow. Specifically, we will concentrate on using potential vorticity to draw conclusions about the coastal jet and use the Davis and Emanuel PV inversion process to identify unbalanced flow. Our three aims:

- Describe the evolution of a CTWR through the lens of potential vorticity.
- Demonstrate that low-level potential vorticity evolution adequately captures the synoptic evolution leading up to a CTWR.

- Use Davis and Emmanuel's PV inversion technique (1991) to distinguish between balanced and unbalanced coastal flow responses.

THIS PAGE INTENTIONALLY LEFT BLANK

# III. DATA AND METHODOLOGY

This chapter describes the data and methodology used to identify and analyze specific cases of CTWRs. A mixture of historical wind reversal cases examined in published articles (from the 1980s and 1990s) and instances of suspected "new" cases (from 2012 and 2013) identified in a time series of coastal buoy observations were utilized. The same reanalysis data was used to analyze both the historical CTWRs and the "new" events.

## A. ACQUIRING CFSR AND PREPARING DOMAIN

For this study, the Climate Forecast System Reanalysis (CFSR) model was used for case selection (new cases) and analysis (all cases). The CFSR is a reanalysis model run at T382 horizontal resolution, using a sigma-pressure hybrid vertical coordinate with 64 levels. Data assimilation depends on historical and operational archives of observations and makes use of raw observed radiance measures from satellite retrievals. Finally, the approximately 50-km resolution of the CFSR dataset is a considerable upgrade from the 383-km resolution data used by Mass and Bond (1996).

The first step was to pull selected CFSR data files from an archive of the full 30-year climatology downloaded at the Naval Postgraduate School. The files are on a global latitude/longitude grid with 0.5-degree resolution at six-hour intervals and contain the full suite of atmospheric parameters. They were re-gridded onto a Lambert Conformal map projection at 25-km resolution over a limited area that includes most of North America. A script was then run to extract a 122 x 130 grid-point sub-domain that enabled us to focus in greater detail on the west coast of California (see Figure 17 for the size of our sub-domain). Despite the desire to focus on a smaller domain, the sub-domain still had to remain of sufficient size in order to capture the larger synoptic pattern coming in from the west-northwest as well as to resolve the complex topography of the California coast.

In order for the data to work with the PV invertibility code, which will be discussed in greater detail in the next section, the CFSR sub-domain also had to truncate the number of vertical levels from 30 to 20 so that the levels had uniform 50-mb spacing.

Although this limits some of the details in the lowest levels, the reduced vertical spacing was only used for the PV inversion.

## B. SELECTING CTWRS

The first set of cases examined were those well documented in published articles. Table 1 contains a list of the six cases studied. The six CTWRs were a mixture of those associated with gravity current dynamics and those forced as a Kelvin wave. In some cases, the subject CTWR was discussed in several papers from different points of view.

Table 1. List of historical CTWRs and associated author(s) of publication.

| Time Period of CTWR | Author(s) of Published Article(s) |
|---|---|
| June 5–6, 1981 | Dorman (1981) |
| May 4–5, 1982 | Dorman (1985); Mass and Albright (1987) |
| May 16–17, 1985 | Mass and Albright (1987); Bond et al. (1995); Mass and Bond (1995) |
| May 8–9, 1990 | Bond et al. (1995) |
| June 10–11, 1994 | Persson (1995); Ralph et al. (1998) |
| July 21–22, 1996 | Nuss et al. (2000) |

For the new cases, CFSR data from the months of July and August of 2012 and 2013 was used. To initially identify potential occurrences of a CTWR between Point Conception to the south and Cape Mendocino to the north, this study utilized a time series of coastal buoy observations; specifically buoy 46013 just north of the San Francisco Bay (see Figure 10 for buoy location). The buoy captured the along- and across-coast components of the wind every six hours and Figures 5 through 8 depict the evolution of the winds for the four months of interest. In the time series, observed winds (red lines) out of the north are shown by a negative number, recorded in meters per second, whereas a shift to southerly wind is noted by a transition to a positive number in meters per second.

To whittle down the list of potential cases, the same criteria used by Mass and Bond (1996) in their climatology of CTWRs was applied, resulting in a search for short periods (1-3 days) of southerly winds (more or less within 45 degrees of the coast) that followed a sustained duration of northerlies. While 2012 provided compelling evidence for five CTWRs spread amongst July and August, the data from 2013 was significantly less straight forward. The first, third, and fifth peaks of the July 2013 time series (see Figure 7) do not appear to have a sustained duration of strengthened northerlies prior to the onset of a period of southerlies. Additionally, there are two brief periods of southerly winds in the August 2013 data that follows a suspected CTWR (see Figure 8). These brief periods did not follow a sustained duration of northerlies and thus, can be discarded. In all, the time series of buoy observations produced 14 potential occurrences of a CTWR.

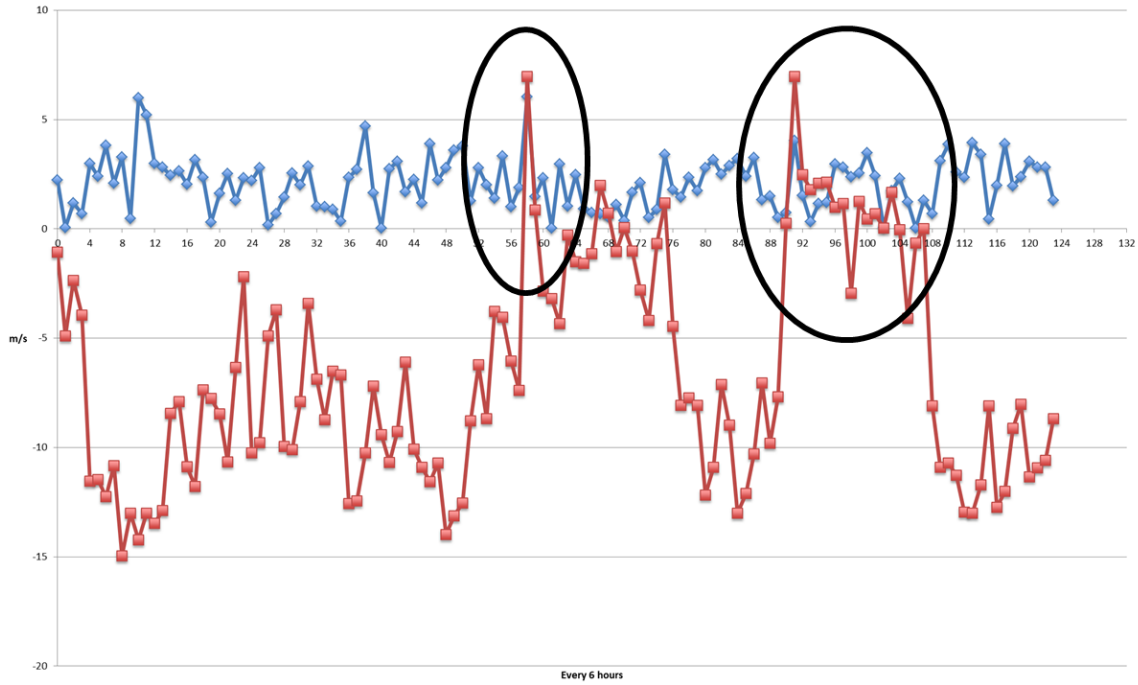


Figure 5. Observed winds (red) from buoy 46013 during July 2012. Two possible occurrences of a CTWR. Blue line is absolute error. Data points along X-axis captured every six hours.

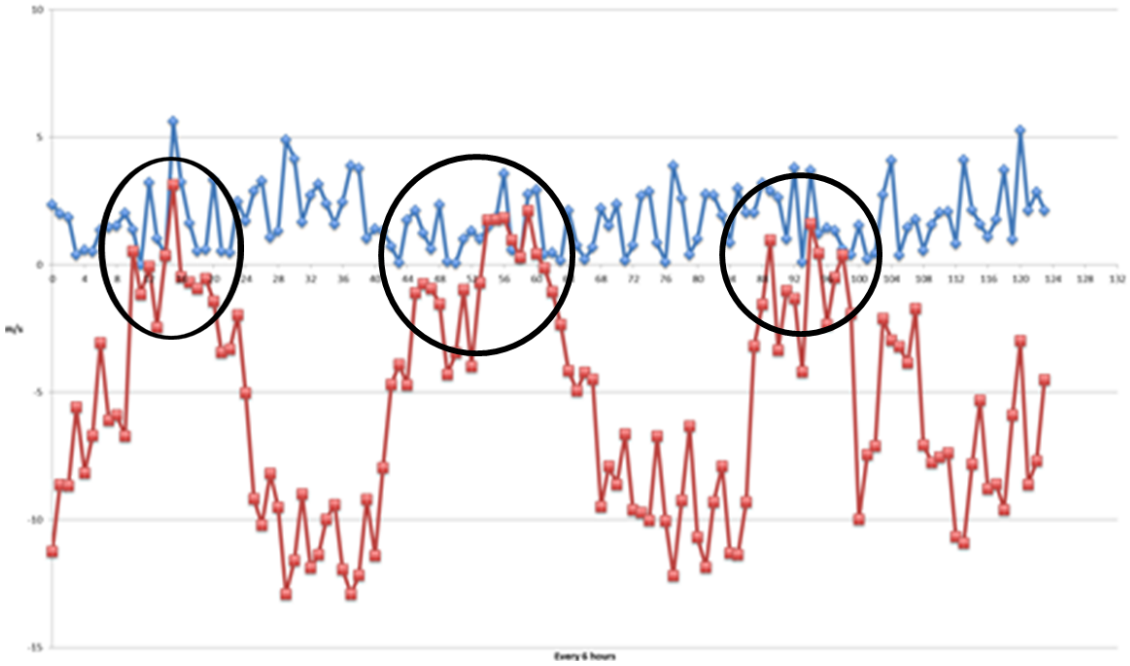

Figure 6. Observed winds (red) from buoy 46013 during August 2012. Three possible occurrences of a CTWR. Blue line is absolute error. Data points along X-axis captured every six hours.

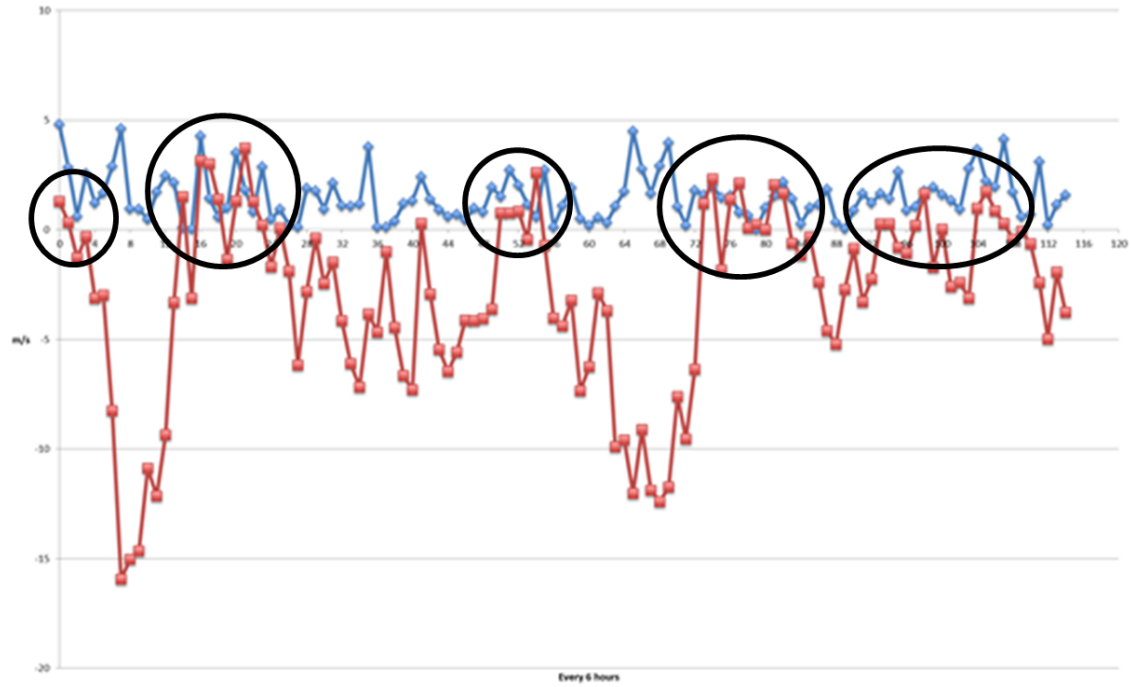

Figure 7. Observed winds (red) from buoy 46013 during July 2013. Five possible occurrences of a CTWR. Blue line is absolute error. Data points along X-axis captured every six hours.

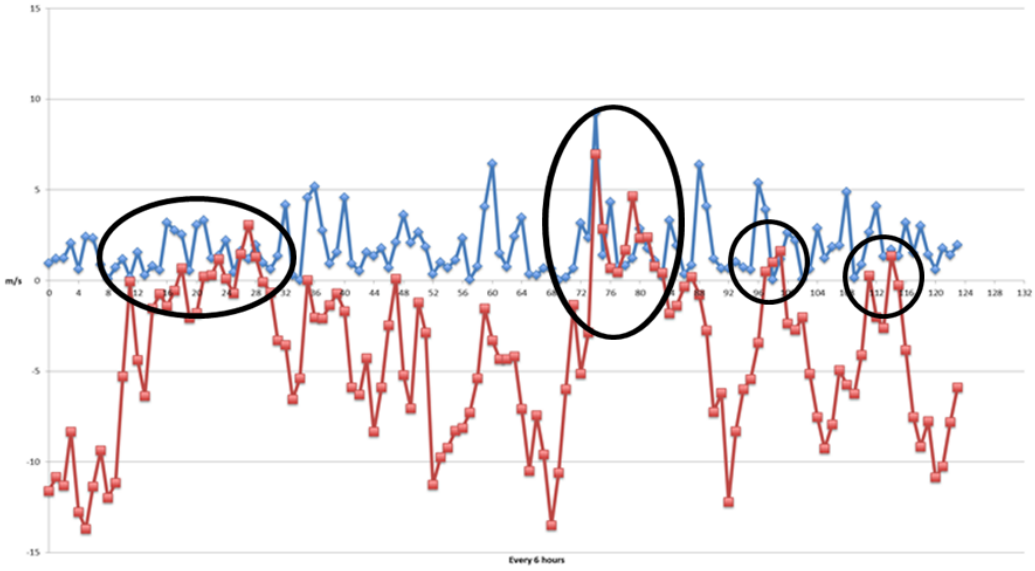


Figure 8. Observed winds (red) from buoy 46013 during August 2013. Four possible occurrences of a CTWR. Blue line is absolute error. Data points along X-axis captured every six hours.

## C. METHODOLOGY

The two goals for this paper were to use potential vorticity to separate balanced wind reversals from those that are an unbalanced flow response (what we refer to as CTWRs) and describe the synoptic environment and evolution necessary to trigger a CTWR (regardless of the dynamics involved). The first task requires the use of the PV inversion technique pioneered by Davis and Emanuel (1991). The second task involved examining six-hourly plots of PV plumes to identify and categorize synoptic patterns associated with a CTWR.

### 1. PV Inversion

To fully utilize potential vorticity as a diagnostic tool, the wind and thermal fields consistent with the observed potential vorticity distribution were retrieved using the PV inversion process introduced by Davis and Emanuel (1991). To invert the potential vorticity distribution, a balance condition between the wind and mass fields must be specified. Davis and Emanuel (1991) used the non-linear balance equation to specify the balance condition. The non-linear balance equation and the definition of potential vorticity are used to form a pair of coupled equations that can be solved for the unique

height and streamfunction fields that fit a given PV distribution and a specified set of boundary conditions. The derived streamfunction gives the winds that are balanced with the PV distribution. These are referred to as the balanced flow or balanced winds.

The code to do the PV inversion was developed at the NPS following the original PV inversion process detailed in Davis and Emanuel (1991). To maintain mathematical consistency in the vertical differencing, the CFSR dataset was resampled at 50-mb spacing in the vertical from 1000 to 50 mb for this computation. The PV was calculated from the observed wind field in the CFSR data for a given time and the surface and upper level potential temperature was extracted to serve as the surface and upper-level boundary conditions to which the retrieved stream function and heights must conform. Lateral boundaries used a fixed in/out flow condition. The code then solves for the stream function and heights in the interior that fit the observed PV distribution and obey the non-linear balance condition. See Davis and Emanuel (1991) for a full description of the process and equations.

One challenge with PV inversion in topography is that because it uses pressure vertical coordinates, the below-ground pressure surfaces were not always self-consistent and caused the solution to diverge in some areas. The divergence results from the mismatch between PV in the below-ground region and the surface (1000 mb) potential temperature field. The mechanics of the CFSR computing winds and temperatures on below-ground pressure surfaces may not be totally self-consistent and lead to problems in the PV inversion process. Consequently, some time periods and cases may have had significant problems.

The results of the PV inversion were used primarily to calculate the unbalanced flow by subtracting the balanced flow from the observed flow. This unbalanced flow then represents flow that is not accounted for by the given PV distribution, which is primarily the synoptic scale flow field. Hence, the unbalanced flow highlights regions where mesoscale processes, friction, or other processes have contributed to flow deviations that are not part of the synoptic scale background (PV-balanced). In the plots that follow, unbalanced flow is illustrated through flow response vectors with large amplitudes while balanced flow is depicted with small-amplitude vectors or even a single dot.

## 2. Characterizing the Synoptic Environment

In order to assist in characterizing the synoptic environment responsible for forcing a CTWR, a series of plots for each of the 20 cases of interest (six historical and 14 "new") were created. For each case, four plots at six-hour intervals over a span of three to five days were generated. A 700-mb plot of geopotential height to gauge the low- to mid-level flow was used, taking particular note of ridging into the Pacific Northwest and troughing extending northwestward out of the valley of central California. Next, plots of sea level pressure and potential temperature (at the surface) were assembled in order to look for the development of an along-coast pressure gradient. The third plot was that of potential vorticity and winds at 950 mb (see Figure 9 for an example). As previously discussed, PV was used as a proxy for the coastal jet and to observe the evolution of winds slightly above the MBL. Finally, the PV inversion code described in the previous section was utilized to plot vectors of the flow response against the geopotential height at 950 mb (in order to see what the "balanced" flow should be).

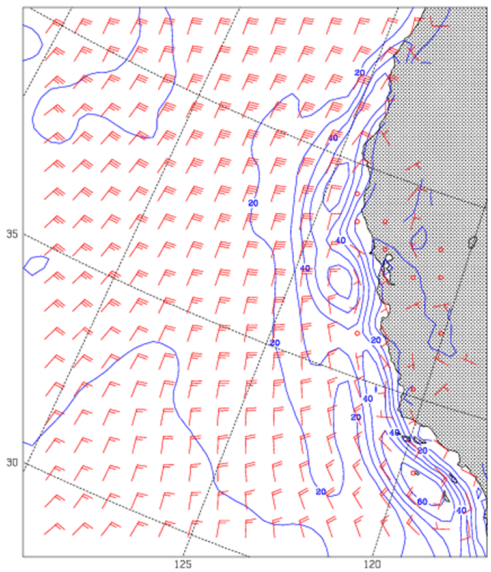


Figure 9. Captured at 1800 UTC on 15 July 2012, a 950-mb plot of potential vorticity (in blue) and winds (in red). A unit of 1 standard PVU (potential vorticity unit) is $10^{-6}$ $Km^2kg^{-1}s^{-1}$. Because PV values are small in the lower atmosphere, PV values were multiplied by a factor of 100. For example, 40 PVU in the plot is represents 0.4 standard PVU.

After formulating the plots, each case was stepped through one six-hour interval at a time; noting how the environment evolved throughout the CTWR. In the historical cases, parameters such as surface pressure and the upper-level flow were examined to ensure their consistency with the published analyses. For all cases, the PV plume was concentrated on in an effort to gain insight into the synoptic conditions that enable a CTWR. The PV structure associated with the CTWR was explored to answer questions such as: is there a critical PVU threshold to trigger a CTWR? Does the PV plume have to separate from the coast to overcome the friction generated by the coastal topography? Finally, the PV plumes were compared with the plots of flow response vectors in order to test the utility of the PV inversion technique; did the plots resulting from the inversion technique truly capture the unbalanced response of a CTWR?

## C. JUNE 1994 CASE STUDY

A notable event from June 1994 (Persson 1995; Ralph at al. 1998; Skamarock 1998; Nuss 2007) was chosen to illustrate the process of using the potential vorticity to characterize the forcing of a CTWR. Since Ralph at al. (1998) provides a detailed analysis of the synoptic situation surrounding the June 1994 CTWR, the case can also be used to calibrate the CFSR and gauge its usefulness for undertaking this study. Observations for the June 1994 CTWR were captured at buoys belonging to the National Data Buoy Center (NDBC) located all along the west coast of the United States (see Figure 10).

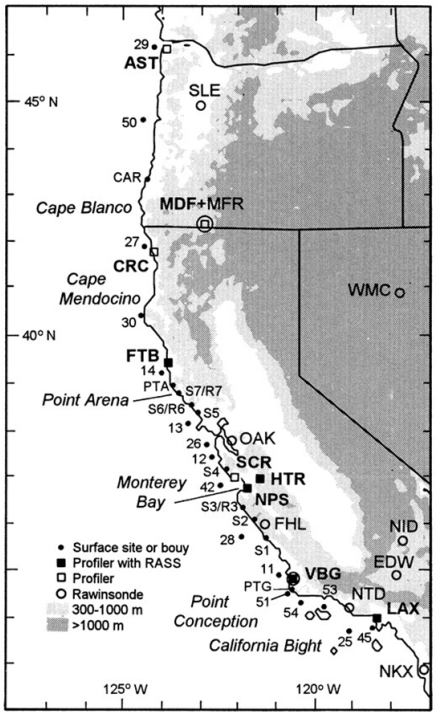


Figure 10. Locations of observing sites and terrain features along the California coast. Buoy numbers xx used here represent buoys numbered 460xx by NDBC (from Ralph et al. 1998).

The 10–11 June CTWR is representative of a strong reversal along the California coast as fog and stratus spread rapidly up the coast starting around 1200 UTC on 10 June (see Figure 3). Due to the propagating nature demonstrated in both satellite and a time series of buoy observations noting the alongshore wind component (see Figure 11), the forcing of the June 1994 CTWR can be attributed to that of a Kelvin wave. Ralph et al. (1998) points out that the synoptic environment closely reflected the Mass and Bond (1996) climatology near buoy 46013 north of San Francisco Bay (see Figure 10). Specifically, a deep-tropospheric ridge over the Pacific Northwest was amplified in the low- to mid-levels while a thermal trough at the surface extended northwestward into the coastal regions of the California/Oregon border, causing an anomalous along-shore pressure gradient with lower pressure to the north. These features were present in the CFSR data as well illustrated by the 700-mb flow (see Figure 12).

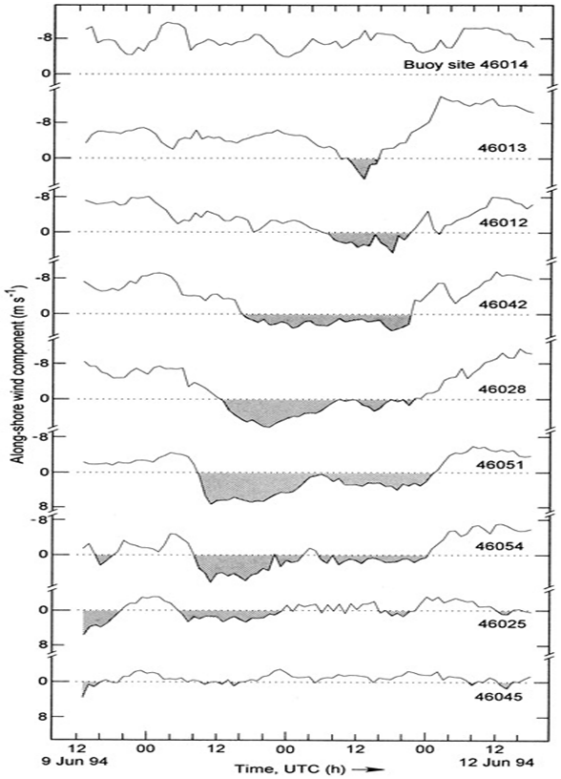


Figure 11. Buoy-observed alongshore wind component ($ms^{-1}$) between 1200 UTC 9 June and 1800 UTC 12 June 1994. Southerly flow is positive, but the velocity scale is inverted so that southerly flow (shaded) appears below the zero line. The northernmost buoy (near Point Arena) is at the top, the southernmost buoy (near Palos Verdes) is at the bottom. Buoy sites are labeled on the right (from Ralph et al. 1998).

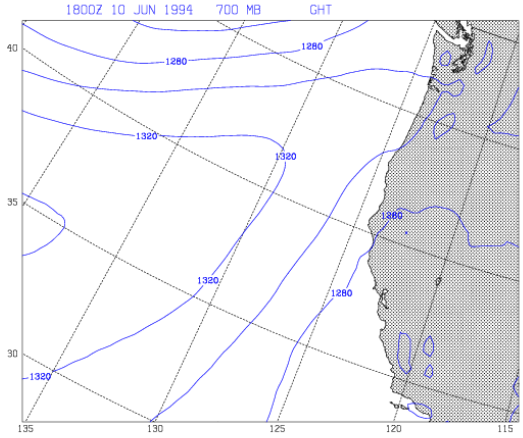


Figure 12. 700-mb flow at 1800 UTC on 10 June 1994 showing a ridge pushing northeastward into Washington and troughing extending northwestward into the coastal region of northern California.

Also crucial to the study conducted by Ralph et al. (1998), and ultimately, their conclusions, was the analysis of a mesoscale low off the California coast that developed south of Monterey Bay and extended southward over a 24-hour period (see Figure 13). Those analyses have been replicated using CFSR data in order to gauge the fidelity of the low-resolution dataset (see Figure 14). Despite the fact that the CFSR analyses resulted in a much smoother surface analysis than the hand-drawn mesoscale analysis of Ralph et al. (1998) the CFSR analysis still managed to reflect the circulation associated with the low-pressure depicted by Ralph et al. (1998) (see Figure 14b) and its subsequent elongation to the southwest at 1200 UTC (see Figure 14c) and 1800 UTC (see Figure 14d). The detailed closed low and mesoscale-high were not distinct in the 50-km resolution CFSR analyses but the surface winds clearly show the CTWR along the coast.

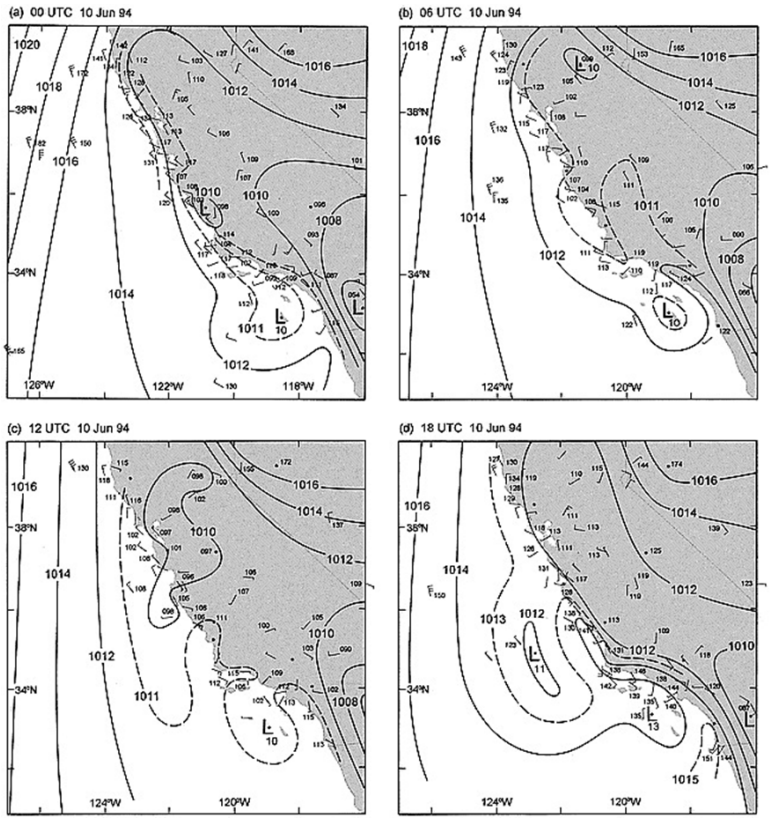


Figure 13. Six-hourly surface observations and SLP analyses (mb) between 0000 UTC and 1800 UTC 10 June 1994. An intermediate pressure contour is shown (dashed). Experimental data from several coastal sites and profiler sates are included, as are standard synoptic observations and ship reports (from Ralph et al. 1998).

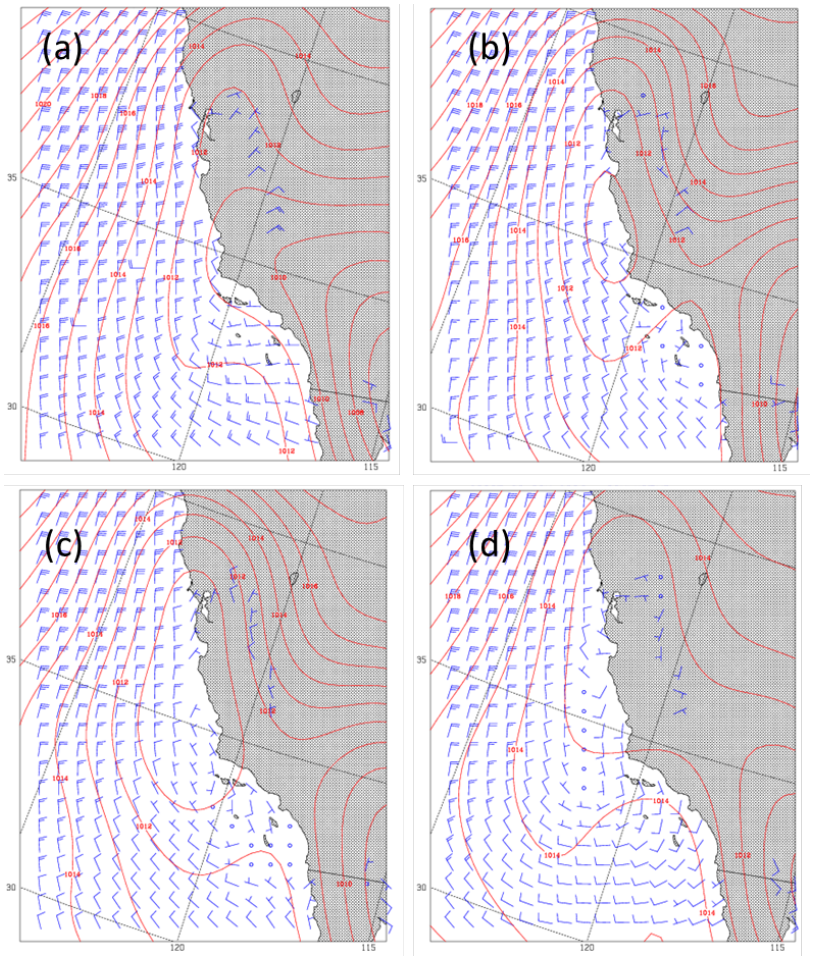


Figure 14. Six-hourly surface observations and sea level pressure analyses (mb) at 0000 (a), 0600 (b), 1200 (c) and 1800 UTC 10 June 1994. Analysis of CFSR dataset is considered a close approximation for observed conditions.

It is clear from Figure 14 that southerly winds of the CTWR started propagating northward around 0600 UTC on 10 June and that time will be used as the onset of the CTWR. In order to understand the role of potential vorticity in the onset of the CTWR, the 950-mb plots of potential vorticity and winds were examined from the 24 hours leading up to the reversal (see Figure 15). From 0600–1800 UTC on 9 June it is evident a weak coastal jet set up as winds above the MBL were 15–18 $ms^{-1}$. In addition, it appears that as the day unfolded, particularly from 1200 to 1800 UTC, the orientation of the winds shifted, becoming slightly more northeasterly and somewhat offshore. Thus, it is

not surprising that the plume of strongest potential vorticity (40 PVU) gradually organized and pushed offshore, following the orientation of the 950-mb winds.

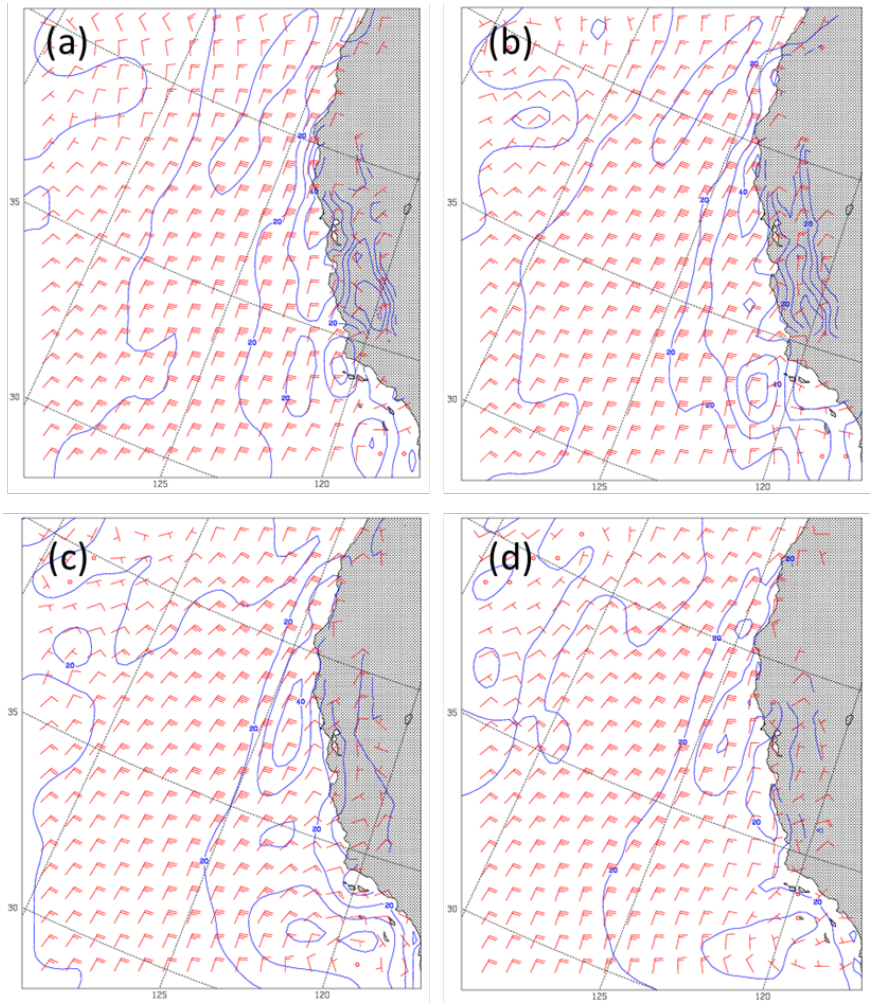


Figure 15. 950-mb winds and potential vorticity at 0600 (a), 1200 (b), 1800 (c) and 0000 (d) UTC 9–10 June 1994. Intervals are every 10 PVU.

As the reversal propagated up the coast on 10 June and into 11 June, the potential vorticity plume that originated from the offshore flow continued to remain strong, organized and pushed off the coast. It is clear that the strongest PV did indeed stay off the coast; indicative of a reorientation of the coastal jet as it was previously hugging the coast at 0600 UTC on 9 June but well off the coast throughout the reversal (see Figure 16). However, it is noteworthy that the PV maximum associated with the reversal itself is

located just off the coast, south of Monterey Bay. This is most evident at 1800 UTC 10 June (see Figure 16c) and the PV maximum does not appear to have advected into the region from the jet. This PV generation is presumably due to the interaction of the Kelvin Wave.

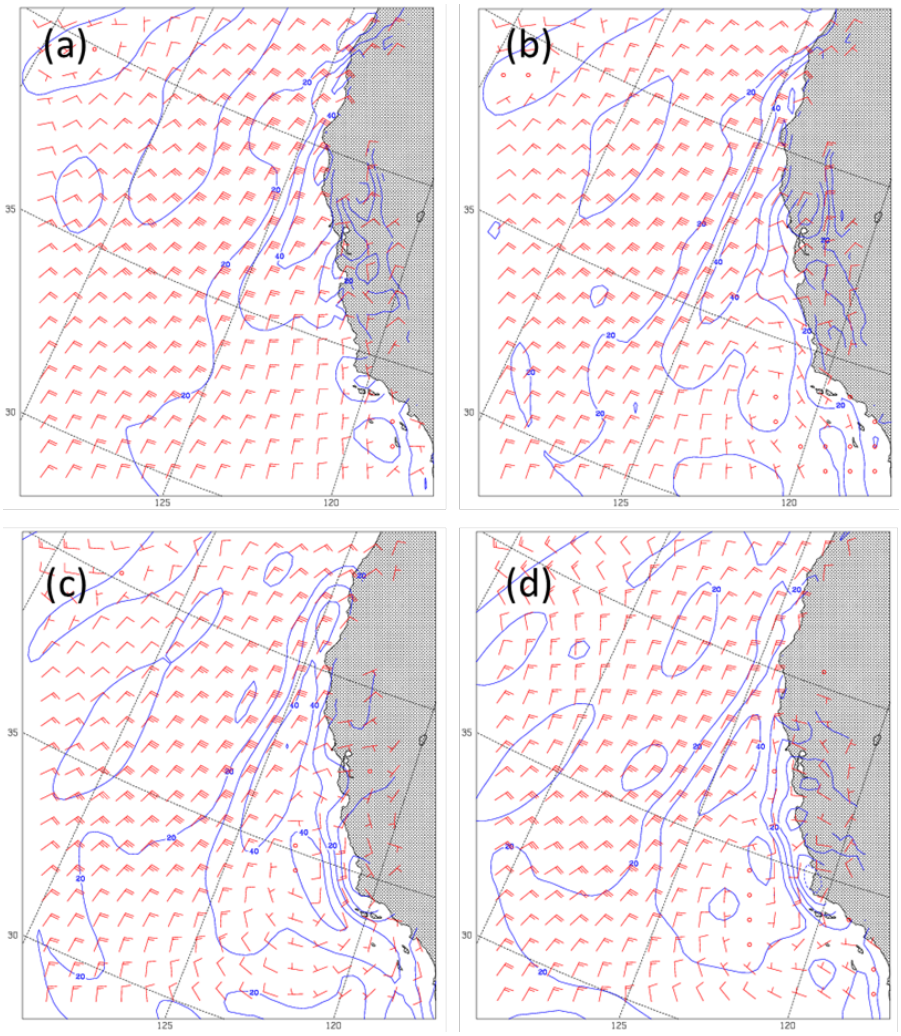


Figure 16. Plots of 950-mb winds and potential vorticity measured in PVU captured at 0600 (a), 1200 (b), 1800 (c) and 0000 (d) UTC 10–11 June 1994.

The next step in our process is taking advantage of the invertibility of potential vorticity by applying the Davis-Emanuel PV inversion technique. Figure 17 shows a series of plots that demonstrate the evolution of the CTWR by depicting the flow

response vectors against the 950-mb geopotential height field. When the flow response vector is relatively small, or absent, it is because the observed winds are in close balance with the PV-derived wind. Although the presence of unbalanced flow response vectors is limited to a small swath along the coast, it is important to remember that a CTWR is a mesoscale feature that occurs on the scale of a few grid points. The 1800 UTC 10 June flow response vectors (see Figure 17b) are relatively large, suggesting that the flow field is unbalanced, generated by processes not in balance with the potential vorticity. Given that this event has been documented to be a Kelvin wave, which is generally a southerly flow out of balance with the potential vorticity, the PV maximum off shore is a response to the Kelvin Wave flow. Also of note, the plot from 1200 UTC 10 June 1994 is absent because of the complexities of dealing with topography described in the "PV Inversion" section. Nevertheless, it is clear in these figures that the June 1994 CTWR was unbalanced in nature and not simply the balanced response to a change in the synoptic environment, as noted by Ralph et al. (1998).

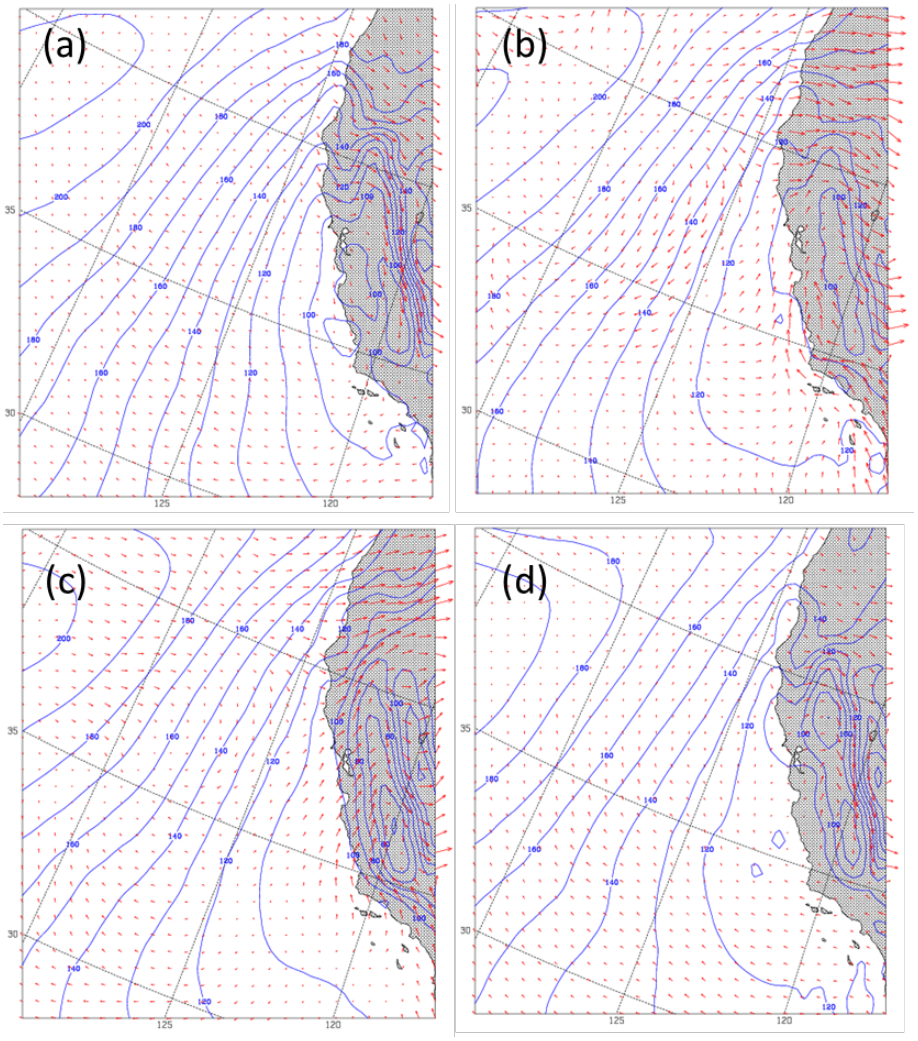


Figure 17. 950-mb geopotential height and flow response vectors at 0600 (a) and 1800 (b) UTC 10 June 1994 and 0000 (c) and 0600 (d) UTC 11 June 1994.

In conclusion, the June 1994 case study demonstrates a few important concepts. First, the CFSR dataset is an improvement in resolution over the 383-km resolution dataset utilized by Mass and Bond (1996) and its usefulness is confirmed through the re-creation of analyses by Ralph et al. (1998). Second, an analysis of the PV plume alone can be sufficient to characterize the synoptic forcing of a CTWR. An evolution of plots leading up to the reversal shows the forming and organizing of a PV plume, and its subsequent reorientation and separation off the coast. This analysis also showed a PV feature associated with the reversal that developed independently of the coastal jet-

derived PV plume. Finally, a look at flow response vectors resulting from an inversion of the PV establishes that this CTWR was a mesoscale, unbalanced phenomena, not solely the balanced flow response to a change in the synoptic environment, and that the mesoscale processes may have generated the PV associated with the reversal.

THIS PAGE INTENTIONALLY LEFT BLANK

# IV. ANALYSIS AND RESULTS

## A. HISTORICAL CASES

Six well-documented CTWRs from the 1980s and 1990s were selected to test the methodology of using potential vorticity to assess the evolution of the synoptic environment and to investigate the hypothesis that the invertibility principle of PV can be utilized to separate reversals that are the result of balanced flow from those that can be attributed to mesoscale influences (unbalanced flow). One of the CTWRs (June 1994) was previously discussed; the remaining five cases will be investigated in this section.

### 1. June 5–6, 1981

On June 5–6, a CTWR progressed around the California Bight at a speed of 5–8 $ms^{-1}$ (Dorman 1985). Deemed a "Catalina Eddy" as the cyclonic reversal confined itself to the California Bight near the Catalina Islands, Dorman (1985) attributed the dynamics of the reversal to that of a Kelvin wave. Although this particular CTWR was limited to a small area, a study of the PV plumes generated during this timeframe may explain why the CTWR did not propagate northward up the coast. Figure 18 shows the evolution of the environment from 1800 UTC on 5 June through 1200 UTC on 6 June.

A look along the northern and central coast of California may be telling of why the reversal did not propagate northward of Point Conception. A potential vorticity plume generated with a max of 40 PVU at 1800 UTC 5 June (see Figure 18a), indicating the presence of a strong coastal jet. Additionally, the jet generated a PV plume that also advected south along the coast, demonstrating the conservative nature of PV. Nevertheless, it is clear that the coastal jet never separated from the coast. In fact, Figures 18b-d show that the PV plume actually moved inland, eliminating any semblance of an across-coast PV gradient. As such, southerly flow north of Point Conception does not develop.

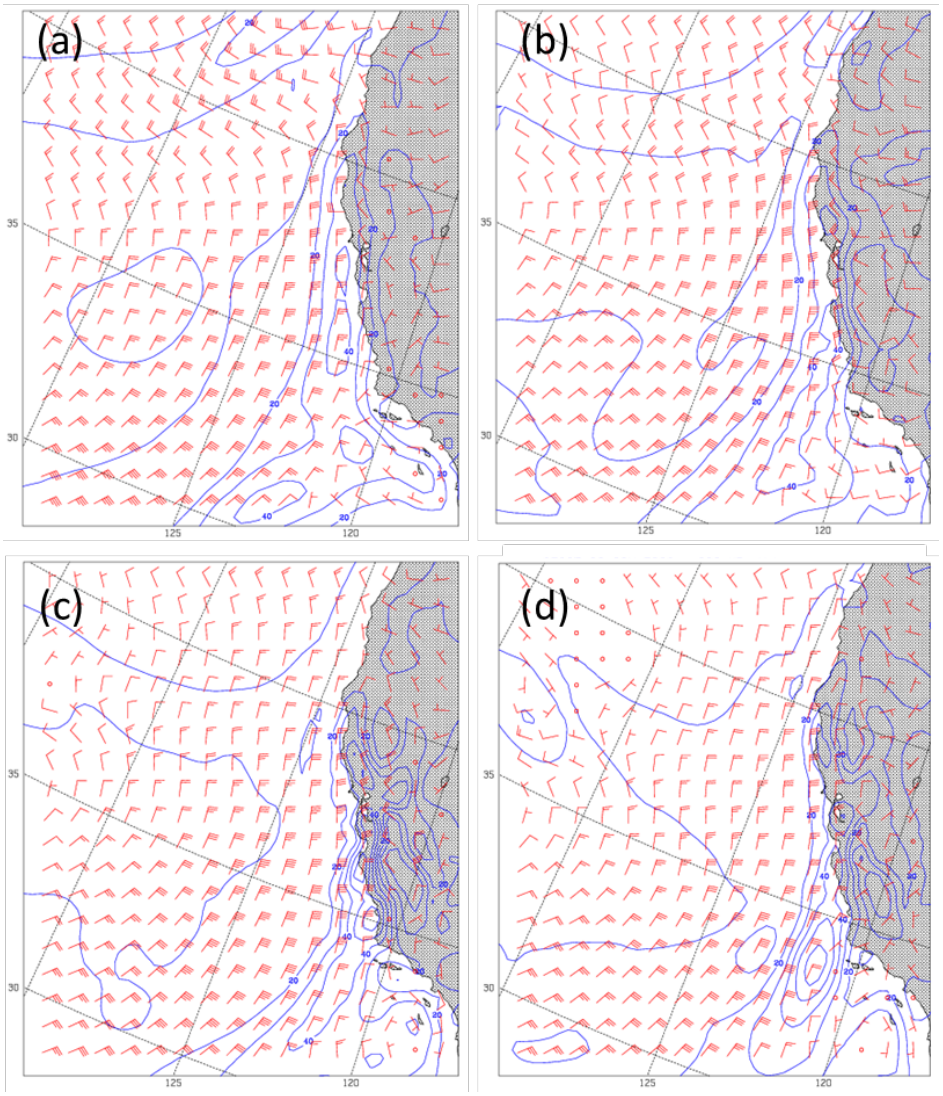


Figure 18. 950-mb winds and potential vorticity at 1800 (a), 0000 (b), 0600 (c) and 1200 (d) UTC 5–6 June 1981.

While the four plots of potential vorticity and 950-mb winds capture the cyclonic nature of the reversal in the California Bight, Figure 18 also depicts the formation of an area of potential vorticity that seems to fit the distribution of winds in the Bight. Therefore, it is not surprising that two plots of flow response vectors from 0000 and 0600 UTC 6 June show relatively balanced flow south of Point Conception (see Figure 19). North of Point Conception, the flow is northerly and well captured by the PV plume along the coast. In the Bight region where the Catalina eddy is occurring, the balanced nature of the flow indicates that the eddy is well depicted by the local PV maximum that

occurs there. Given that the eddy is a balanced flow response, the lifting of the MBL and movement of stratus that occurred would have been due to advection; a notion dismissed by Dorman (1985).

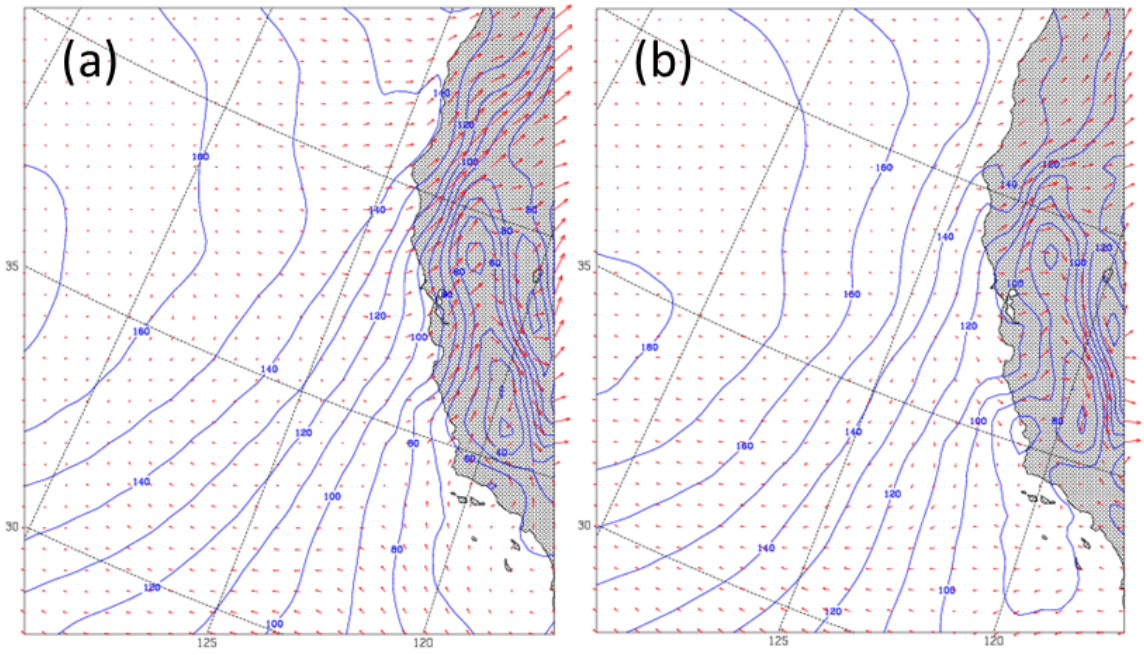


Figure 19. 950-mb geopotential height and flow response vectors for 0000 (a) and 0600 (b) UTC 6 June 1981.

### 2. May 4–5, 1982

May 1982 also produced a CTWR that started from a Catalina Eddy. However, this reversal stands in stark contrast to the CTWR from June 1981 as, starting the afternoon of 3 May, it propagated quickly up the coast of California. While Dorman (1985) published an in-depth examination of this CTWR and concluded that it was the work of a Kelvin wave, an alternate view provided by Mass and Albright (1987) is that the CTWR was controlled by the alongshore pressure gradient created by the synoptic scale flow. The May 1982 CTWR is classic as it featured abrupt wind shifts recorded in observations and soundings along the coast and a sharp leading edge of fog/stratus visible in satellite imagery. The PV plumes generated by the northerly flow in the day leading up

to the release of the CTWR illustrate one reason why this CTWR may have differed from that of June 1981.

Figure 20 depicts the evolution of potential vorticity along the coast of northern California for the 18-hour period beginning at 0600 UTC 3 May and leading up to the release of the CTWR northward from Piedras Blancas (approximately 0000 UTC 4 May). At 0600 UTC (see Figure 20a) a PV maximum occurs at the coast, north of San Francisco. By 1800 UTC May 3 (see Figure 20c), this PV maximum has moved south to Monterey Bay and the well-defined PV plume exists to well south of Point Conception. At the same time, it appears that the coastal jet has started to shift its orientation, particularly north of Cape Mendocino, producing alongshore flow instead of onshore flow. By 0000 UTC 4 May (see Figure 20d), the coastal jet shifts further still, producing slightly more offshore flow and shifting the PV seaward. Throughout 3 May, though the coastal jet reoriented slightly and the plume of PV advected southward, it is not apparent that the PV plume had yet to separate definitively from the coast or establish an across-coast PV gradient.

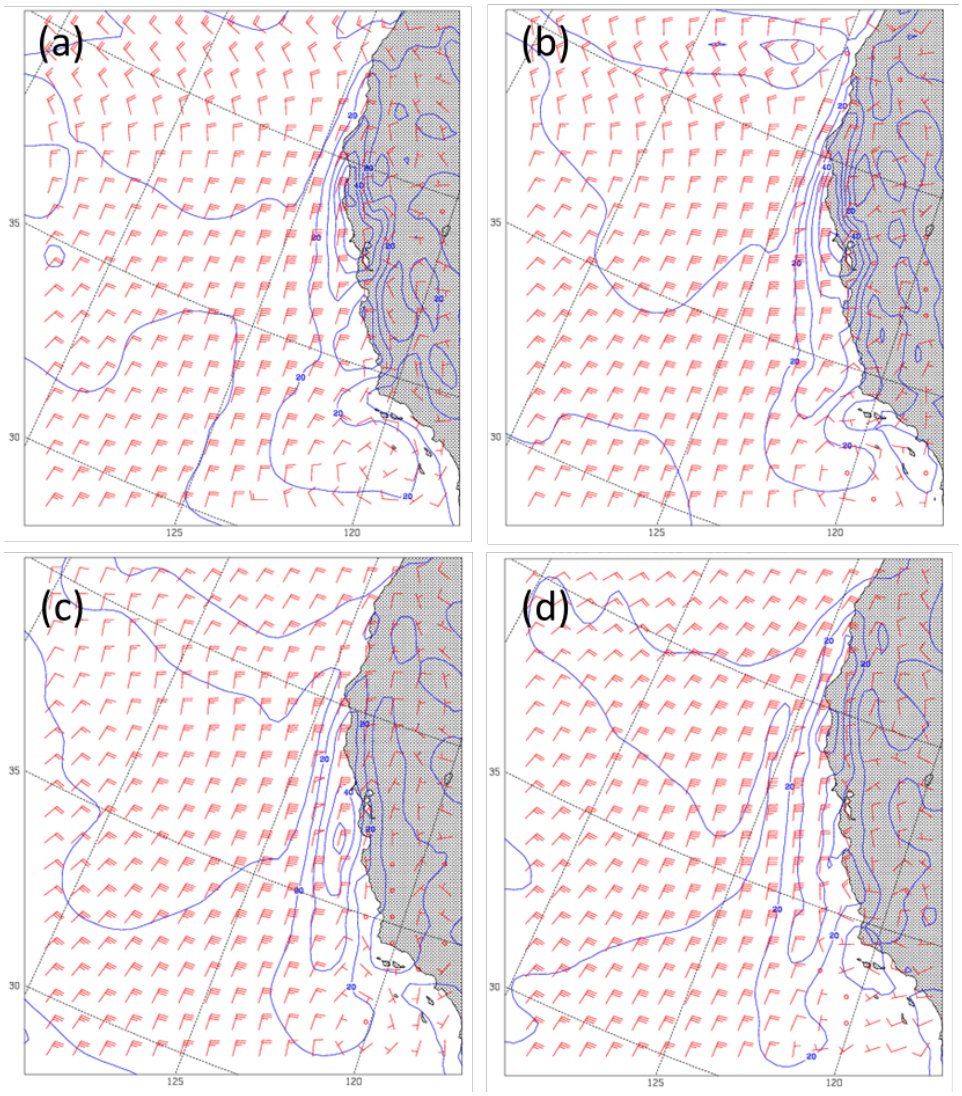


Figure 20. 950-mb winds and potential vorticity at 0600 (a), 1200 (b), 1800 (c) and 0000 (d) UTC 3–4 May 1982.

Over the next 24 hours, from 0000 UTC 4 May, the situation changed as the PV plume pushed offshore and the CTWR propagated northward. The CTWR pushed north swiftly and brought southerly winds to Monterey Bay by 1500 UTC 4 May and a narrow tongue of stratus to San Francisco's shores by 01 UTC 5 May (Mass and Albright 1987). Figure 21 shows how the PV plume and associated across-coast PV gradient enabled the CTWR to propagate northward. Specifically, Figure 21c shows the PV maximum relocated dramatically offshore, northwest of San Francisco Bay, by 1800 UTC and even further offshore, due west of San Francisco Bay at about 125W, by 0000 UTC 5 May. At

the same time, the northerlies on the western side of the coastal jet intensified, creating even more PV which supports a stronger southerly flow near the coast that may have enabled the CTWR to overcome the topographically-induced friction and propagate northward.

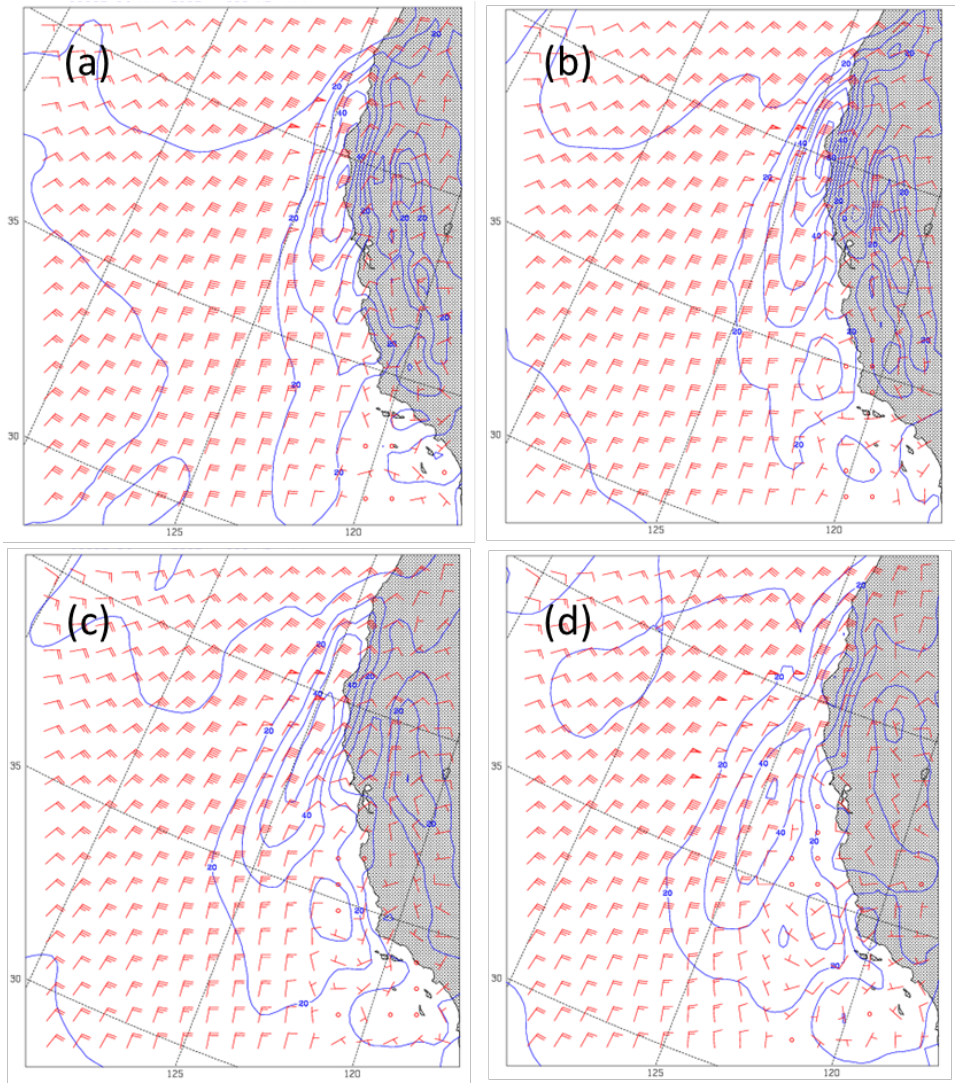


Figure 21. 950-mb winds and potential vorticity at 0600 (a), 1200 (b), 1800 (c) and 0000 (d) UTC 4–5 May 1982.

The May 1982 CTWR is also noteworthy in that it demonstrates characteristics similar to the June 1994 case. From 1200 UTC 4 May through 0000 UTC 5 May (see Figures 21b-d), a region of potential vorticity was produced that seems to be a separate

entity from the PV originated through the offshore flow of the coastal jet. As in the June 1994 case, it is presumed here that the generation of a secondary potential vorticity maximum can be attributed to the CTWR itself.

Beginning at 1800 UTC 4 May, it is clear that a portion of the flow along the coast of California, stretching from the Bight northward into San Francisco Bay, is somewhat out of balance with the flow that should have derived from the PV in the area (see Figure 22a). However, as the CTWR generated its own area of PV, it stands to reason that the reversal would have become more in balance with the PV-derived flow. Still, the unbalanced flow is about the same. As such, the flow response vectors in Figure 22b show an unbalanced flow along the coast. The magnitude of the flow response is somewhat less than six hours earlier, suggesting a trend toward more balance. Nevertheless, by utilizing the Davis Emanuel PV inversion technique it can be concluded that the CTWR is not the geostrophically-balanced result of a change in the along-shore pressure gradient.

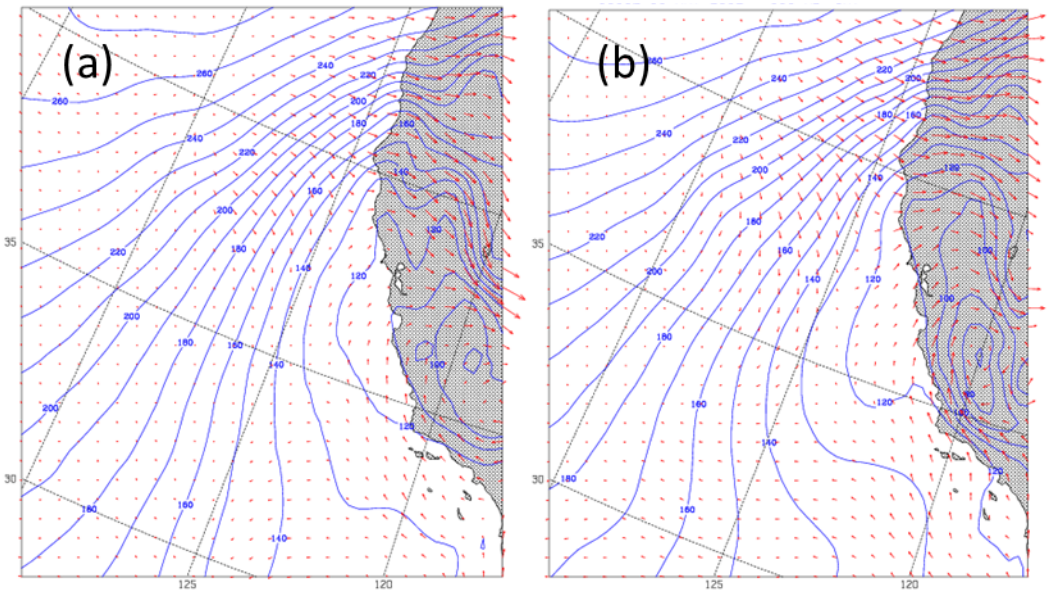


Figure 22. 950-mb geopotential height and flow response vectors at 1800 (a) and 0000 (b) UTC 4–5 May 1982.

### 3. May 16–17, 1985

Although the May 1982 CTWR displayed a rapid temporal transition from northerly to southerly winds as it propagated northward, it is still considered a "weak" wind reversal in terms of wind strength (Mass and Albright 1987). On the other hand, Mass and Albright (1987) provide a detailed examination of another reversal that is typified as a "strong" CTWR—May 1985. The May 1985 reversal also differs from the previous two cases in that it originated much further north, in the vicinity of the Monterey Bay vice the California Bight, as evidenced by a tongue of coastal stratus stretching into San Francisco by 2100 UTC 15 May (Mass and Albright 1987). One interesting facet of this particular CTWR is that the disturbance pushed northward all the way through Oregon and Washington on 17 May and into British Columbia by 18 May. A plot of 950-mb winds and PV at 0000 UTC 17 May shows a large swath of southerlies reaching the California/Oregon border (see Figure 23) while Mass and Albright (1987) noted that the stratus tongue associated with this reversal reached southern Oregon by 1900 UTC 16 May.

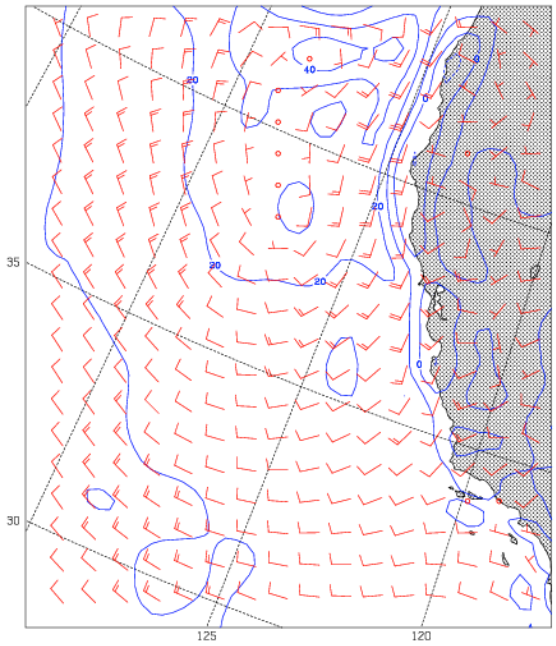


Figure 23. 950-mb winds and potential vorticity at 0000 UTC 17 May 1985.

A look at the potential vorticity plumes on 15 May echoes earlier findings that, as the reversal pushed up the coastline, the coastal jet shifted its orientation, intensified, and separated from the coast; creating an across-coast PV gradient. At 0000 UTC 15 May (see Figure 24a), 18 to 21 hours before the reversal encased the San Francisco Bay with fog and stratus, an area of PV started to generate due to the shifting of the coastal jet to produce slightly offshore flow. Six hours later (see Figure 24b), persistent offshore flow by the low-level jet resulted in a stronger, more defined plume of potential vorticity with northerlies strengthening to 25 $ms^{-1}$ and a PV maximum of 60 PVU encamped atop Cape Mendocino. By 1200 UTC 15 May, the PV maximum pushed offshore (see Figure 24c). Finally, as the CTWR was starting to push northward toward San Francisco Bay about 1800 UTC (see Figure 24d), the PV plume bulged westward, driving the PV maximum noticeably offshore, creating space for the reversal to move up the coast.

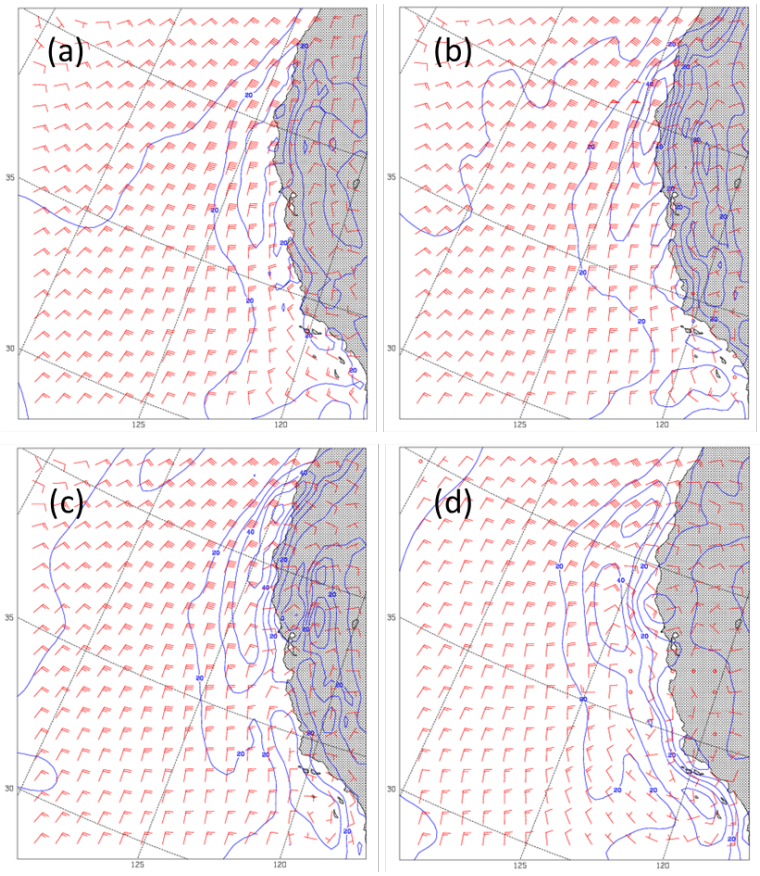


Figure 24. 950-mb winds and potential vorticity at 0000 (a), 0600 (b), 1200 (c) and 1800 (d) UTC 15 May 1985

While the May 1985 event underscores the hypothesis that separation of the coastal jet is necessary to the formation and/or propagation of a CTWR north of Point Conception, the same event demonstrates some of the shortcomings of utilizing the PV inversion technique. Figure 25 compares plots of PV plumes and 950-mb winds with those containing flow response vectors derived from the PV inversion process. At 0000 UTC 16 May (see Figure 25a) and 0600 UTC 16 May (see Figure 25c), it is clear that the CTWR is in full swing as southerlies have made their way to Cape Mendocino. It is also clear that there was very little difference between the environment at 0000 and 0600 UTC; southerlies dominated the coastal region with the presence of a strong across-coast PV gradient extending from the Bight to Point Arena. Because of the similarities in the PV plumes, it is expected that plots of the associated flow response vectors should be similar. Unfortunately, Figure 25b depicts a large area of unbalanced flow along the coast while Figure 25d shows remarkably balanced flow just six hours later. While it is possible that the PV inversion code is temperamental and should be used with caution, it is also possible that the difference in the flow response can be attributed to diurnal effects altering the static stability of the atmosphere as 0000 UTC is the warm part of the day while 0600 UTC is during the night.

Later in its life cycle, the May 1985 CTWR stands out from the other reversal events in that it appears to evolve from a mesoscale feature into a large system reflected into the upper levels. At 1800 UTC 15 May, close to the time of the onset of the CTWR near San Francisco Bay, a closed low in the 700-mb geopotential height field moved off the coast of northern California (see Figure 26). The feature remained a fixture in the 700-mb flow for the next 48 hours as the system transited northward.

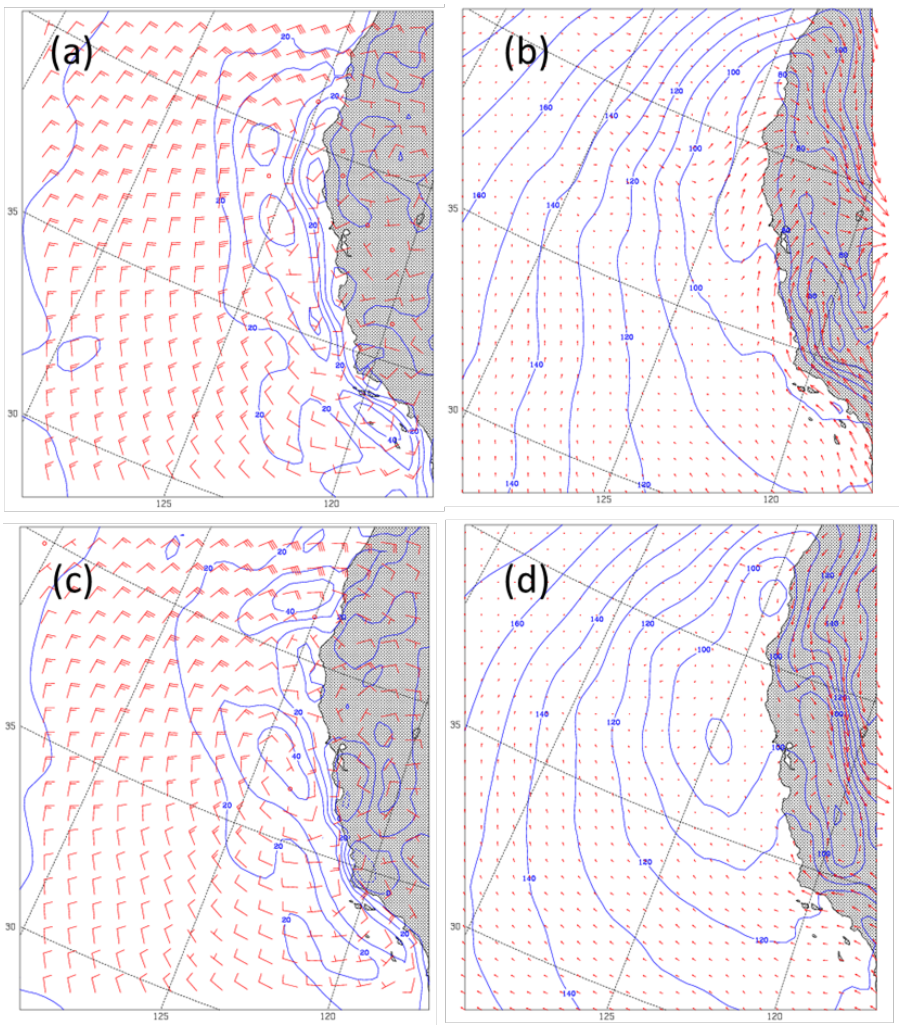


Figure 25. 950-mb winds and potential vorticity at 0000 (a) and 0600 (c) UTC and 950-mb geopotential height and flow response vectors at 0000 (b) and 0600 (d) UTC 16 May 1985.

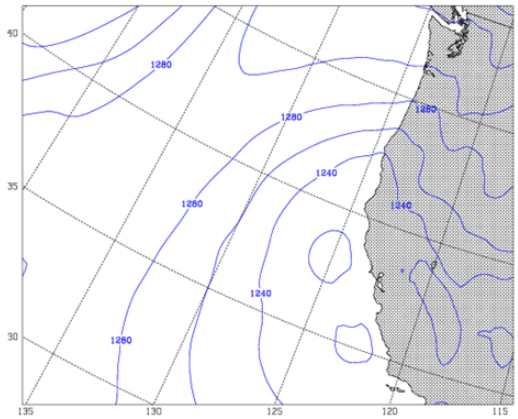

Figure 26. 700-mb geopotential height at 1800 UTC 15 May 1985.

### 4. May 8–9, 1990

Bond et al. (1996) used the May 1990 CTWR event to illustrate how the reversal adheres to the synoptic climatology they established through their 10-year study. Figure 27 shows the eastern Pacific high situated to the west-northwest of Washington and Oregon. Additionally, the surface analysis depicts ridging pushing into Washington with a distinct thermal trough, oriented from southeast to northwest, pushing through the coastal mountain range and offshore. A surface buoy just south of the trough axis also shows slightly higher surface pressure, suggestive of the anomalous along-shore pressure gradient required to trigger a reversal.

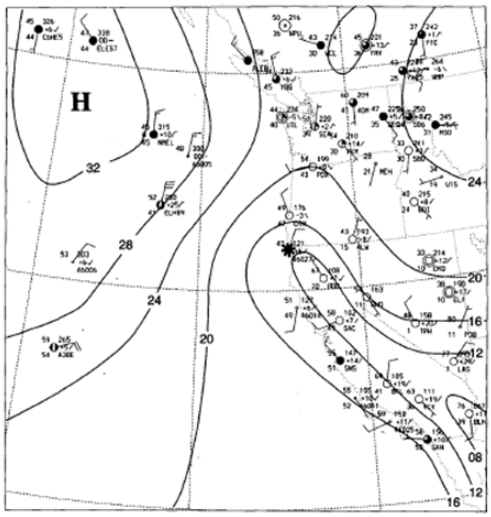


Figure 27. NCEP surface analysis for 0600 UTC 9 May 1990 (from Bond et al. 1996).

The May 1990 CTWR may have generated as early as 0600 UTC 8 May in the California Bight as indicated by the presence of a small, cyclonic circulation and area of potential vorticity (see Figure 27a). However, southerly winds did not make their way north of Point Conception until sometime between 1200 and 1800 UTC 8 May (see Figures 27b-27c). The evolution of the PV-plume structure leading up to and including the release of the CTWR sometime around 1500 UTC 8 May is very similar to the cases previously discussed. At 0600 UTC, a relatively strong low-level coastal jet (25 $ms^{-1}$) with a slight offshore orientation created a PV plume with a maximum of over 60 PVU

(see Figure 27a). At the same time, a second area of PV existed in the Bight; associated with a small area of cyclonic turning. Around 1200 UTC (see Figure 27b), the area of maximum PV located between Cape Mendocino and San Francisco Bay elongated and pushed ever so slightly off shore. Six hours later, by 1800 UTC 8 May (see Figure 27c), the PV plume moved completely offshore, though the maximum weakened to 40 PVU. Nevertheless, the movement of the PV plume westward enabled the establishment of an across-coast PV gradient that spurred southerlies to quickly move north of Monterey Bay before turning easterly in the San Francisco Bay.

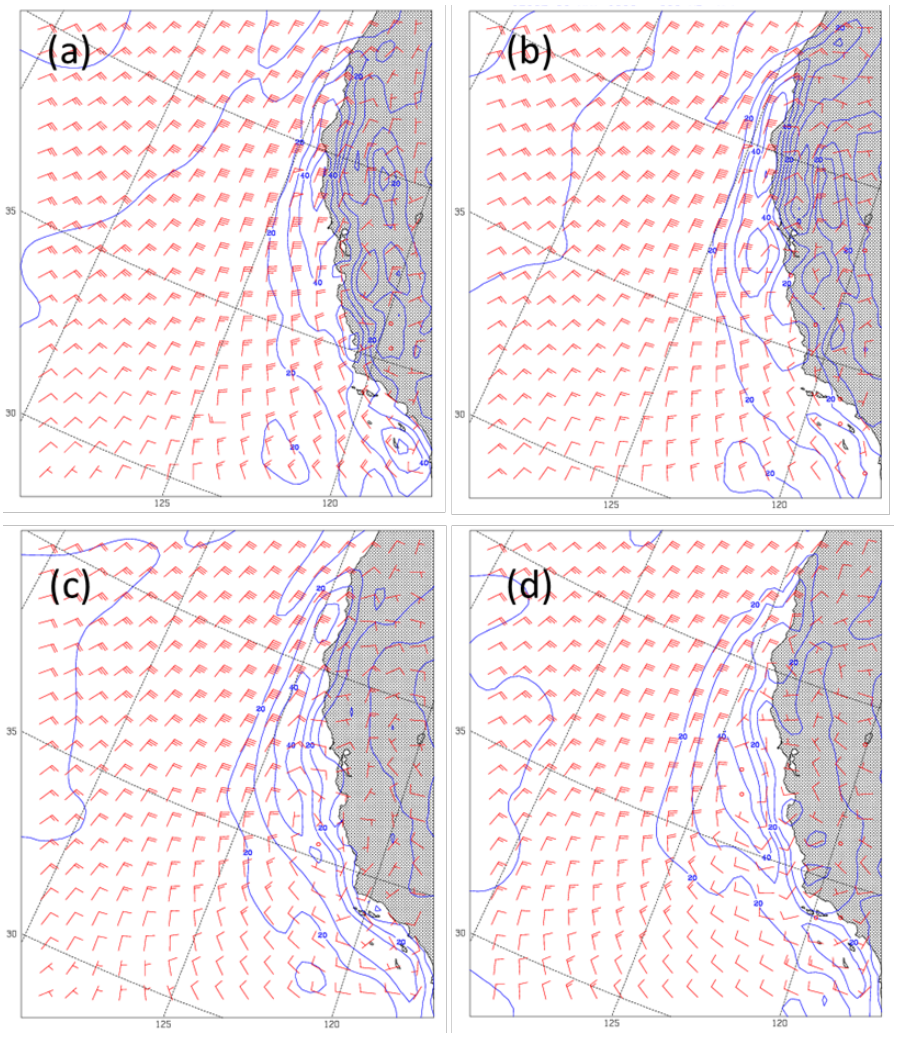


Figure 28. 950-mb winds and potential vorticity at 0600 (a), 1200 (b), 1800 (c) and 0000 (d) UTC 8–9 May 1990.

Though not as widespread an event, the May 1990 CTWR shares similarities with the May 1985 reversal. Both CTWRs differed from the June 1994 case in that the southern extension of their PV plumes did not maintain a northeast-southwest orientation. Rather, their respective plumes, after bulging westward with a PV maximum in the vicinity of 125W, turned back to the southeast to follow the coastline. In all three cases, however, it is important to note that, although the orientations of their respective PV plumes differed, they all moved seaward of the coastline and established an across-coast PV gradient. The May 1990 CTWR is similar to the May 1985 reversal in another way. After the reversal reached the San Francisco Bay area, it appeared to evolve into a synoptic-type feature, reflected by its PV signature, as it continued its propagation northward (see Figure 29). The cyclonic circulation in Figure 29d, west of San Francisco, is over 500 km wide, suggesting a more synoptic-scale structure than a feature trapped within a Rossby Radius of the coastline.

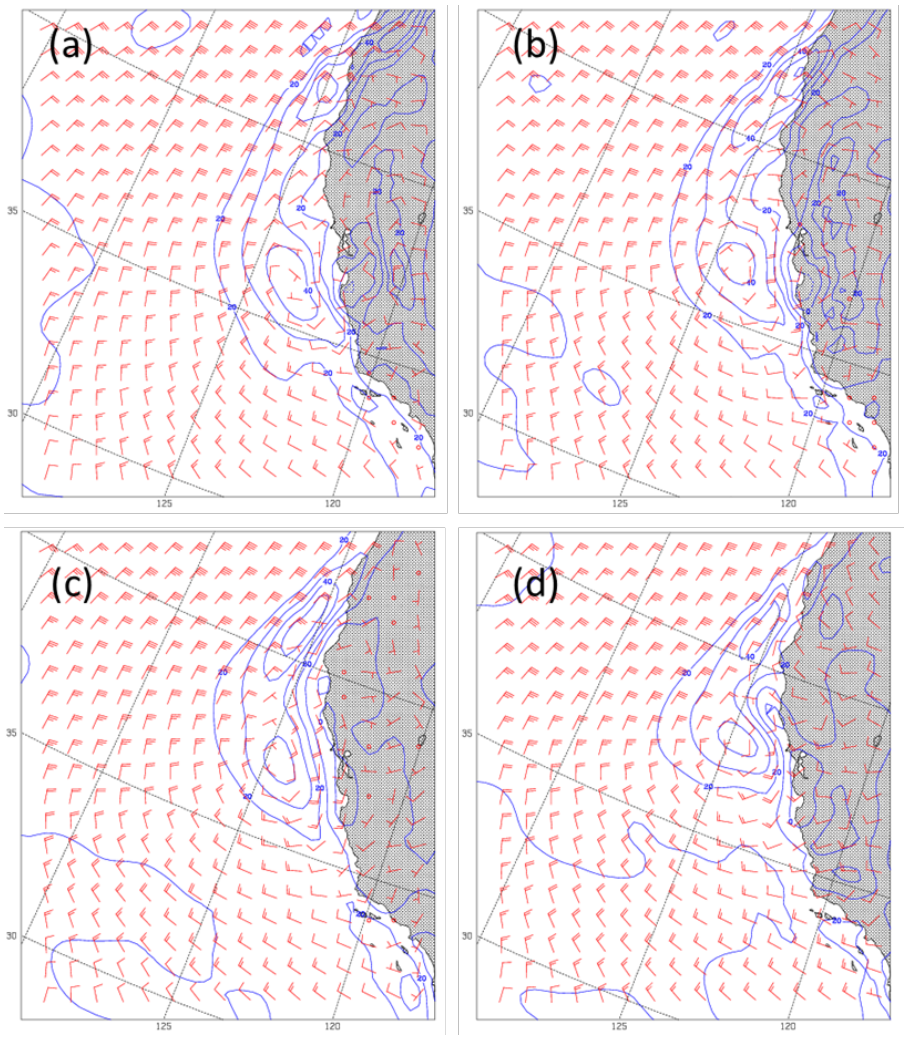


Figure 29. 950-mb winds and potential vorticity at 0600 (a), 1200 (b), 1800 (c) and 0000 (d) UTC 9–10 May 1990.

While it looks as if the reversal is in balance with the PV distribution, analysis of the flow response vectors advocates the reality of unbalanced flow along the coast. Before the onset of the CTWR, at 1200 UTC 8 May (see Figure 30a), the coastal flow was relatively balanced with a small sampling of unbalanced flow in the Bight. By 1800 UTC (see Figure 30b), the flow response vectors resulting from the PV inversion depict weak unbalanced flow pushing northward along the coast. This result marries nicely with the timing of the reversal and observed southerlies (see Figure 27c). At 0000 UTC 9 May (see Figure 30c), the PV inversion works well to capture the unbalanced nature of the reversal as the flow response vectors are of significant magnitude. Moreover, it seems

that the largest concentration of unbalanced flow is north of San Francisco Bay, again accurately portraying the propagation of the CTWR. Interestingly, by 0600 UTC (see Figure 30d), the flow response vectors indicate increasingly balanced flow. While this might be a result attributable to diurnal effects, the CTWR might also have been in the process of attaining balance as it started to transition into a synoptic-scale system.

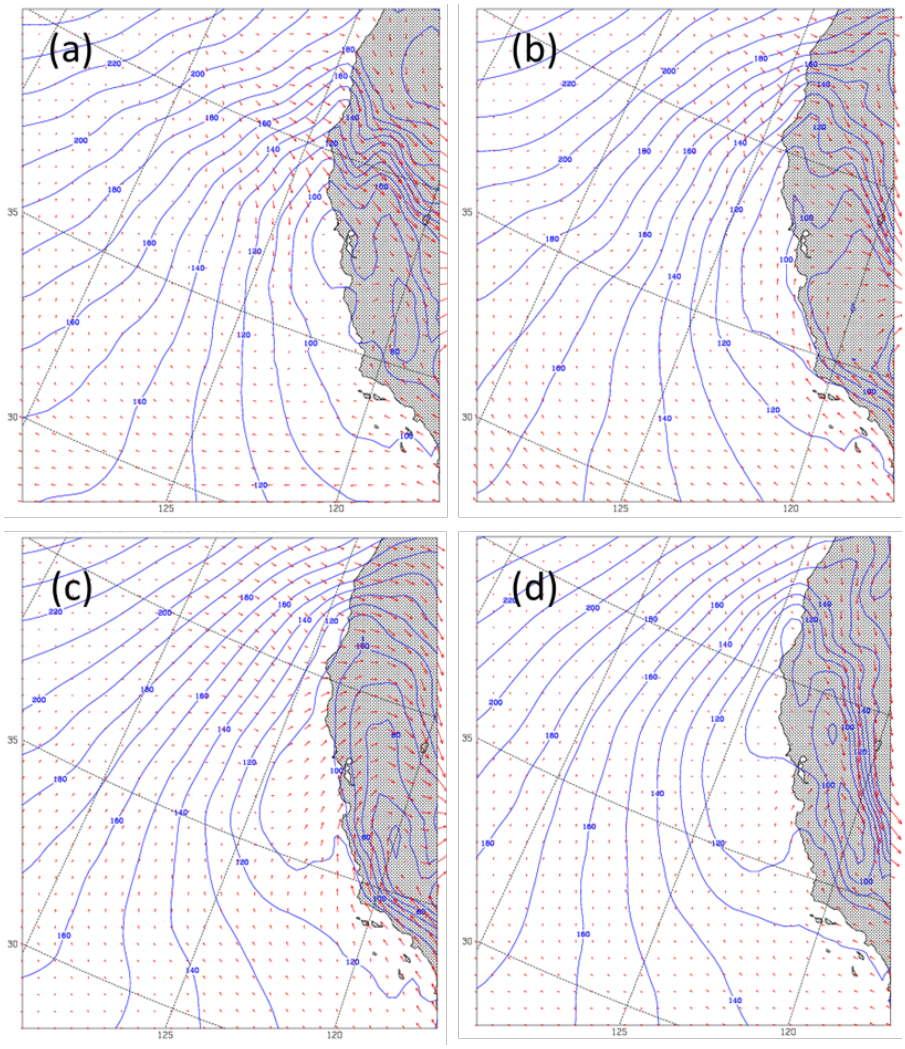


Figure 30. 950-mb geopotential height and flow response vectors at 1200 (a), 1800 (b), 0000 (c) and 0600 (d) UTC 8–9 May 1990.

### 5. July 21–22, 1996

Observed as part of the 1996 Experiment on Coastally Trapped Disturbances (ECTD) field program, a CTWR from July 1996 demonstrated a similar synoptic setup to the June 1994 event in that surface analyses revealed a mesoscale offshore low near San Francisco and a coastal pressure ridge (see Nuss et al. (2000) Figure 13). However, the July 1996 CTWR did not feature the same clarity in its propagation of fog and stratus (Nuss et al. 2000). Like the May 1985 CTWR, the southerly flow of the July 1996 reversal originated north of Point Conception, in the vicinity of San Luis Obispo Bay, and started its northward propagation around 1500 UTC 21 July. An analysis of the PV distribution in the 24 hours leading up to the release of the CTWR yields insight into the interesting evolution that emphasizes the ability of PV to be used as a parameter to characterize the event.

At 1200 UTC 20 July (see Figure 31a), an area of PV developed in the California Bight and hints at the formation of a cyclonic circulation; perhaps a Catalina Eddy. At the same time the coastal jet was generating potential vorticity south of Cape Mendocino as the flow interacted with the mountainous terrain. However, stronger than normal easterly flow around the Catalina Islands (perhaps due to the early presence of the PV) at 1800 UTC (see Figure 31b) produced still more potential vorticity in the area. The generation of PV is particularly evident at 0000 UTC 21 July as a PV maximum of nearly 60 PVU generated in the Big Sur region, south of Monterey (see Figure 31c). The development of PV in that area along the coast blocked any chance of an across-coast PV gradient from setting up; leading to the return of northerly flow through the Bight (see Figure 31d).

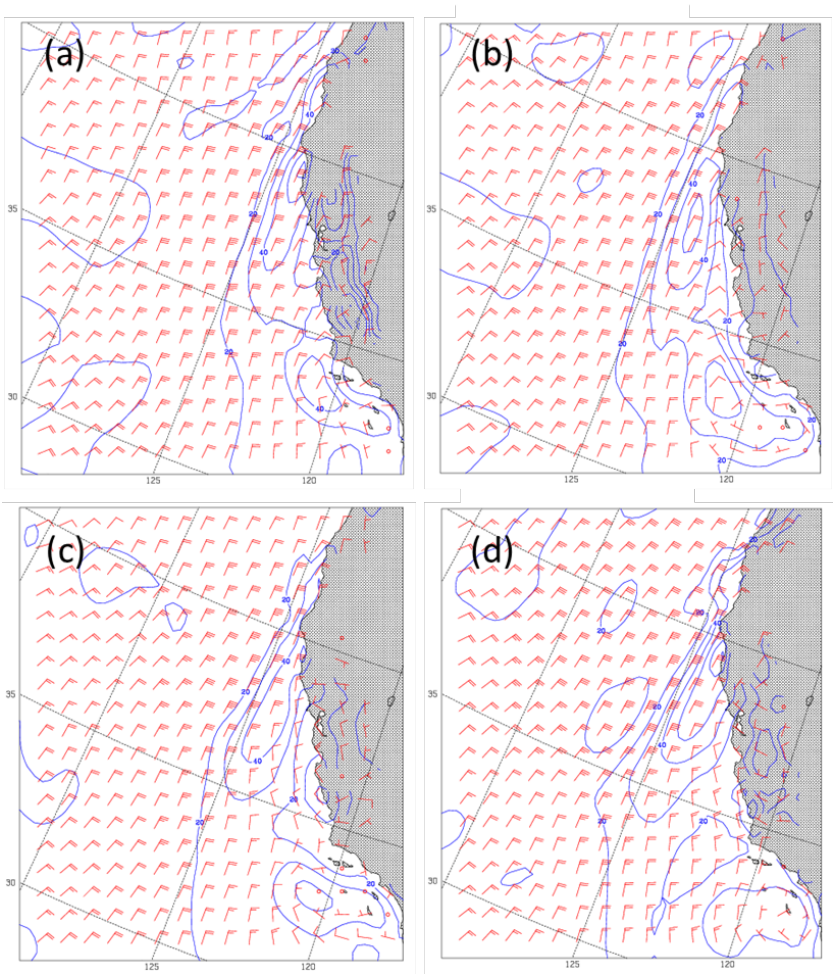


Figure 31. 950-mb winds and potential vorticity at 1200 (a), 1800 (b), 0000 (c) and 0600 (d) UTC 20–21 July 1996.

Despite the false alarm on 20 July, the CTWR was able to take shape and propagate northward of Point Conception by 1200 UTC 21 July (see Figure 32b). Starting at 0600 UTC 21 July (see Figure 32a), the PV distribution characterizing the environment surrounding the CTWR was similar to many of the cases previously discussed. Throughout 21 July and into 22 July, the low-level coastal jet clearly shifted to produce more offshore flow, generating a stronger, more organized PV plume in the process. This CTWR emphasizes once again that the formation of an across-coast PV gradient is necessary to the reversal's ability to propagate northward. Figure 32c shows the PV maximum pushed well off the coast and at 0000 UTC 22 July the PV plume assumed the bulging shape characteristic (see Figure 32d) previously observed.

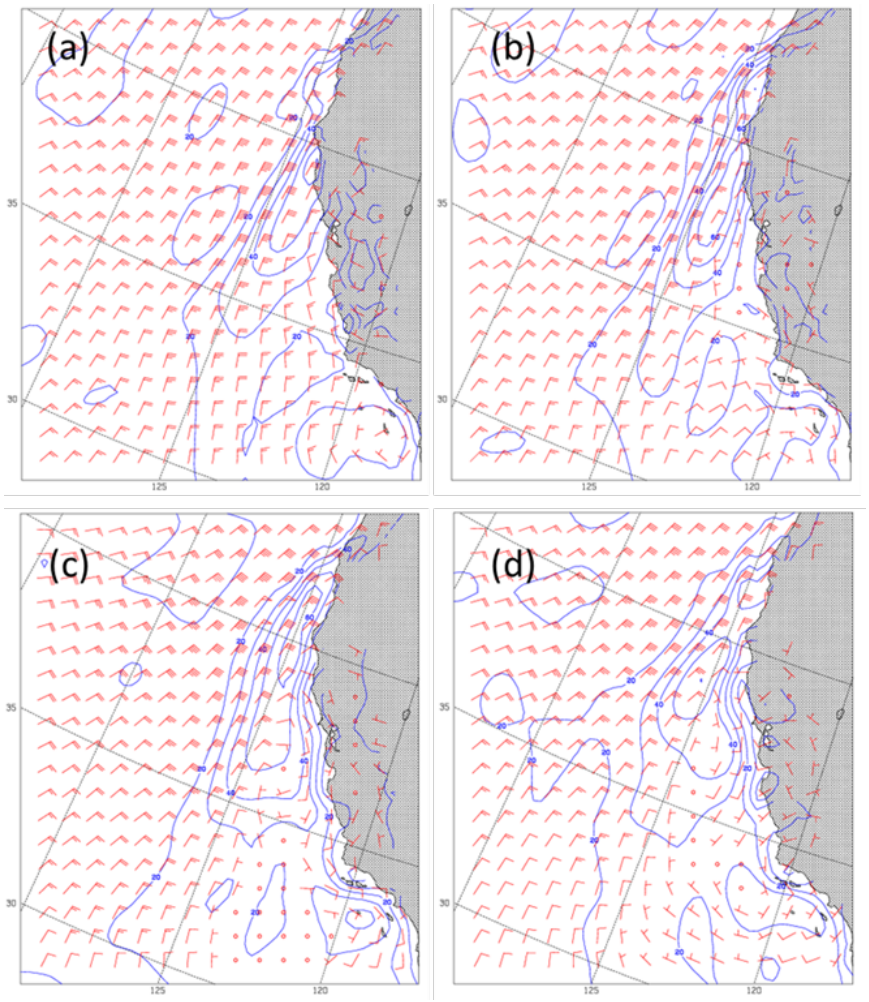


Figure 32. 950-mb winds and potential vorticity at 0600 (a), 1200 (b), 1800 (c) and 0000 (d) UTC 21–22 July 1996.

This CTWR equally illustrates some of the strengths and weaknesses of applying the Davis Emanuel PV inversion technique. At 1200 UTC 21 July, a plot of flow response vectors shows relatively balanced flow (see Figure 33a); appropriate as the CTWR had yet to begin its journey northward. Regrettably, the next plot of flow response vectors is not available until 0000 UTC 22 July, 12 long hours later. By this time a definite unbalanced flow along the coast from the Bight to Cape Mendocino is evident, well past the CTWR initiation. This highlights a few shortcomings of the PV inversion technique. The first shortcoming of the technique is a result of CFSR data being limited to being available at only six-hour intervals. As the lifespan of a CTWR can be very short, the usefulness of the CFSR dataset can be limited. Despite the limited availability

of the CFSR dataset, there is a 12-hour gap in the generation of flow response vectors (instead of just six hours) because the PV inversion code used to generate the vectors is very sensitive to topographical influences (as discussed in the background section of this paper) and was numerically unstable at 1800 UTC 21 July.

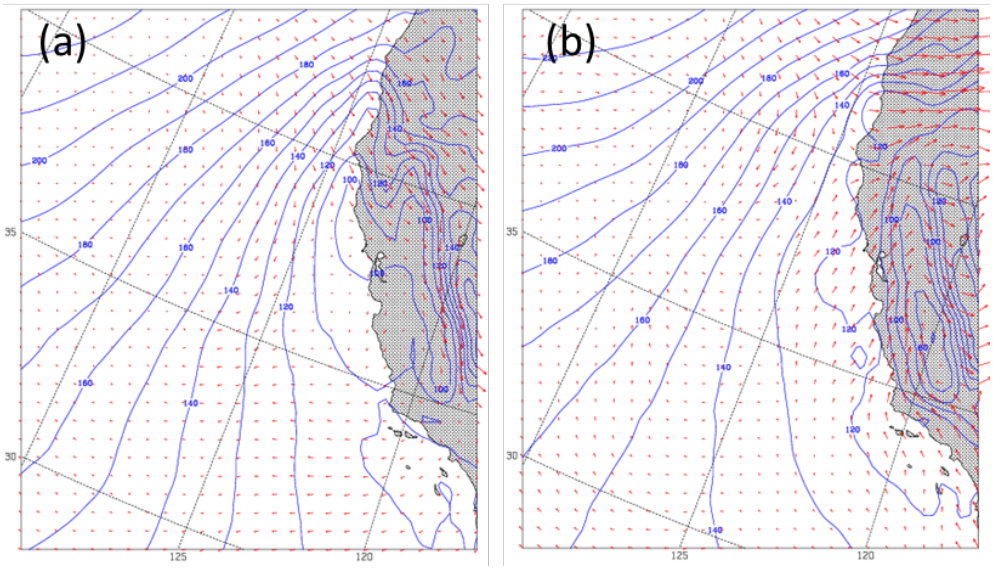


Figure 33. 950-mb geopotential height and flow response vectors at 1200 (a) and 0000 (b) UTC 21–22 July 1996.

## B. RESULTS FROM HISTORICAL CASE ANALYSIS

A study of the six historical cases yields a number of encouraging results regarding the use of potential vorticity to characterize the synoptic environment surrounding a CTWR. At the same time, use of the Davis Emanuel PV inversion technique to identify balanced and unbalanced coastal flow responses to the PV produced varying results.

First, using the PV plume as a proxy for the coastal jet proved to be a useful technique that produced consistent results. In each of the historical CTWR events analyzed in this study, the low-level coastal jet played a determining role in whether or not the CTWR propagated northward of Point Conception. Out of the six cases, five propagated northward up the California case. In the sixth case, the CTWR remained confined to the California Bight. In the propagation cases, the analysis of PV plumes

indicated a shifting jet that produced increased offshore flow. Additionally, propagation in each case only occurred once the PV maximum separated from the coast and the PV plume established an across-coast PV gradient. The June 1981 CTWR event demonstrated the inability of the reversal to transit north of Point Conception as the area of PV associated with the jet failed to adequately displace from the coast.

This study of potential vorticity also demonstrated that the orientation of the PV, and by proxy the orientation of the coastal jet, was not as critical in enabling a CTWR as was its separation from mountainous terrain. In some of the cases, the PV plume associated with the coastal jet separated from the coast and advected to the south-southwest, away from the coastline. In other cases, however, the PV maximum bulged westward while the southern extension of the plume retained an alongshore orientation. In either of these situations, the CTWR was able to propagate northward.

A third result that was clear in some cases but not as apparent in others was the generation of a secondary PV maximum in the immediate vicinity of the CTWR itself. Although potential vorticity is a conserved quantity that should not be generated in the absence of friction or diabatic processes, it appears that, in a few cases, a CTWR was able to generate an area of PV along its western flank. While the reversal may have started out as an unbalanced flow response associated with Kelvin wave or gravity current dynamics, on occasion the CTWR developed an area of potential vorticity that seemed to enable it to attain a degree of balance with the atmosphere.

Finally, the PV inversion process resulted in flow response vectors that successfully captured both balanced and unbalanced flow. Overall, the results stemming from the PV inversion technique were not as consistently conclusive as was the analysis of PV plumes. In many instances, the CTWR showed up clearly as unbalanced flow. Yet in other cases, such as the CTWR from May 1985, the relatively unchanged atmosphere (as identified by its area of potential vorticity) produced two plots over a six-hour period of drastically different flow response vectors. Additionally, the PV inversion process also seemed to capture the CTWRs transition from unbalanced to balanced flow as the reversal evolved into a synoptic-scale system. This result is evidenced particularly well by the May 1990 CTWR.

## C. APPLICATION OF RESULTS TO "NEW" CASES FROM 2012/2013

The methodology used to study the six historical CTWR events was applied to the 14 potential cases identified in the time series of buoy observations gathered from the summers of 2012 and 2013 (see Figures 5–8). An understanding of the low-level potential vorticity evolution is sufficient to characterize the synoptic environment required to enable a CTWR and should work for any cases of wind reversals. To emphasize that point, the PV fields surrounding a sample of the 14 suspected reversals are presented here.

Buoy 46013 showed a strong transition to southerly winds around 1200 UTC 15 July 2012 after a period of sustained northerlies (see Figure 5). A plot of the potential vorticity and 950-mb winds produced a similarly sharp transition as Figure 34a shows that southerlies had yet to arrive north of San Francisco by 1200 UTC but were prevalent up the California coast by 1800 UTC (see Figure 34b). More importantly, it is clear from Figure 34 that the PV max associated with the coastal jet was predominately off shore at 1800 and 0000 UTC 15–16 July but increasingly onshore by 0600 UTC, demonstrating once again that the establishment of an across-coast PV gradient is necessary for a CTWR. By 0600 UTC 16 July, the coastal jet shifted to onshore flow and the PV plume likewise pushed inland, ushering in a return to northerly flow.

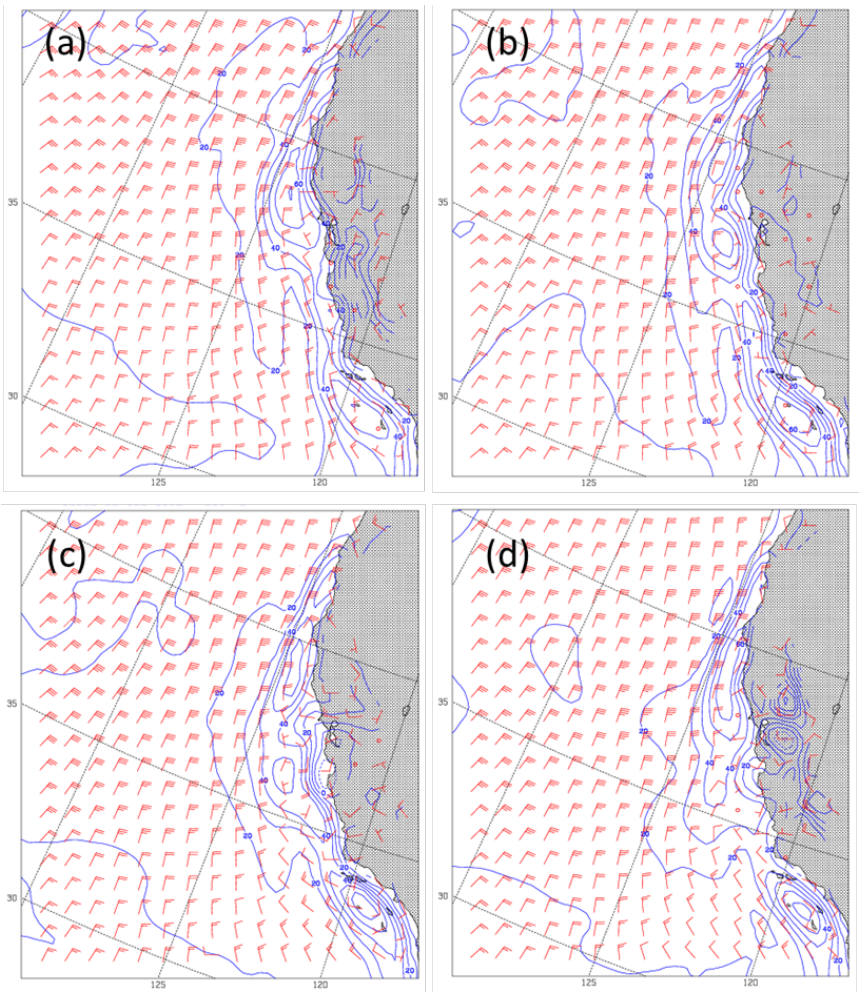


Figure 34. 950-mb winds and potential vorticity at 1200 (a), 1800 (b), 0000 (c) and 0600 (d) UTC 15–16 July 2012.

Around 22 July 2012, buoy 46013 shows a rapid transition to southerly winds followed by several oscillations of northerly and southerly flow (see Figure 5). This pattern is captured in plots of 950-mb winds and PV as well. At 1200 UTC, a strong PV maximum organized just west of Point Arena and northerly flow dominated the coast, though a reversal appeared to be forming as a Catalina Eddy in the Bight (see Figure 35a). Six hours later, southerlies made their way all the way up the coast in a very narrow swath and into San Francisco Bay (see Figure 35b). From a PV standpoint, the maximum does not appear to move much further offshore, however, the across-coast PV gradient increases which may have provided enough forcing to overcome the friction. However,

an area of PV along the Big Sur coast and San Simeon does appear to push westward from 1200 to 1800 UTC, setting up an across-coast PV gradient in that area.

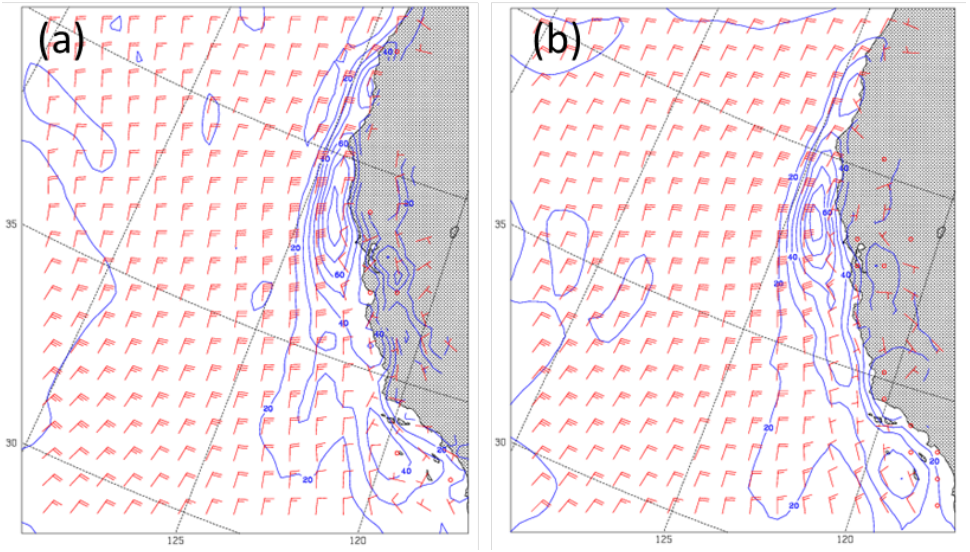


Figure 35. 950-mb winds and potential vorticity at 1200 (a) and 1800 (b) UTC 22 July 2012.

Towards the end of August 2012, a wind reversal, albeit weak, is clearly evident in observations at Buoy 46013 (see Figure 6). An analysis of 950-mb winds, however, does not endorse the presence of a CTWR. Four plots, beginning at 0600 UTC 24 August, show that southerly winds indicative of a reversal are present only at 1800 UTC (see Figure 36c) as northerlies return to the California coast by 0000 UTC 25 August (see Figure 36d). Keeping in mind the Mass and Bond (1996) requirement that southerly winds must remain for at least 12 hours following the transition from northerlies, the case for this event to be a CTWR can be rejected. A look at the PV plumes and evolution of the coastal jet during the same time frame perhaps explains why the CTWR event did not truly unfold. Figures 36a and 36b show a strong, organized PV plume synonymous with the low-level coastal jet. Additionally, the PV maximum associated with the jet does appear to be stationed just off the coast. Nevertheless, the coastal jet does not seem to reorient or separate from the coast over the next 24 hours and introduction of southerlies is only brief.

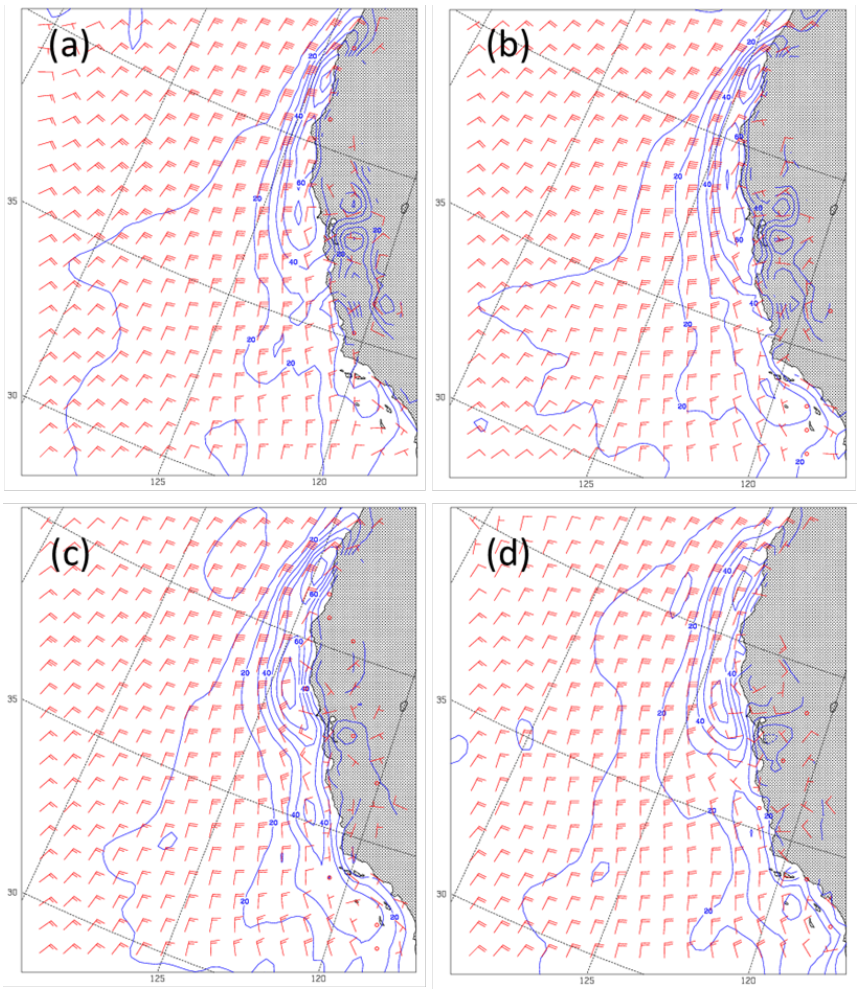


Figure 36. 950-mb winds and potential vorticity at 0600 (a), 1200 (b), 1800 (c) and 0000 (d) UTC 24–25 August 2012

Buoy 46013 signals the possibility of five reversal events in July 2013. Each of the possible cases presents a unique PV structure that does not echo the classic evolution of a CTWR event repeated throughout the historical cases previously examined. Throughout the possible July 2013 cases, a common theme emerged—very strong PV maxima (on the order of 80–100 PVU) with very little separation from the coast. Additionally, two of the timeframes developed wind reversals further north than previously examined; originating north of the San Francisco Bay. The events displayed southerly winds associated with the coastal-jet derived PV plume while northerlies controlled the coastline south of San Francisco. Figure 37a illustrates such a case from 0000 UTC 10 July 2013 while Figure 37b captures a similar reversal event five days later

at 1800 UTC 15 July. Both CTWRs demonstrated a split-PV structure with little to no potential vorticity in the vicinity south of Monterey Bay, enabling southerly winds north of San Francisco while northerlies otherwise remain in place.

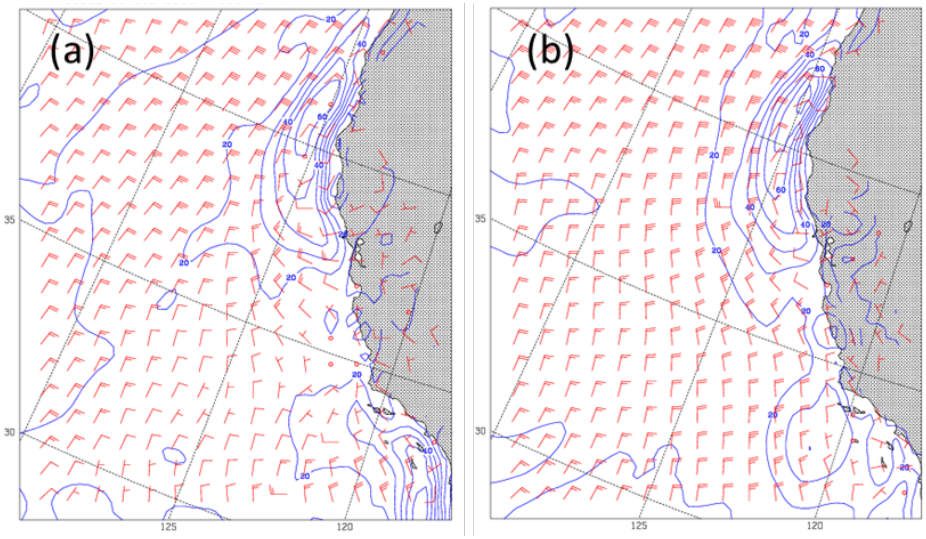


Figure 37. 950-mb winds and potential vorticity at 0000 UTC 10 July 2013 (a) and 1800 UTC 15 July 2013 (b).

July 2013 also introduced cases where a CTWR clearly takes place in the wind field despite no separation from the terrain by the coastal jet. 30 July is one example where the coastal jet does not appear to assume much of an offshore orientation or push its PV maximum westward. In fact, it seems as if a slight onshore flow may have developed at 1800 UTC north of Cape Mendocino (see Figure 38b). Nevertheless, the CTWR was able to make its way into the San Francisco Bay. One reason is that, even though the jet did not separate, the atmosphere still established a very strong across-coast PV gradient from the Monterey Bay south to Point Conception. The PV gradient was so strong that the plots in Figure 38 depict 0 PVU along the coast in the midst of southerly winds. In addition, as the PV maximum strengthened from 1200 to 1800 UTC, large-scale westerly flow increased toward the coast; perhaps due to the stronger across-coast PV gradient.

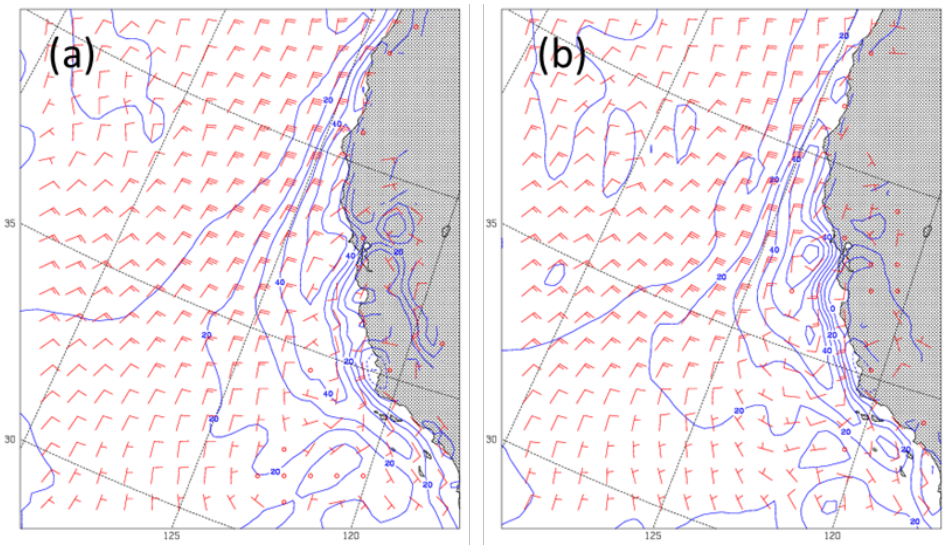


Figure 38. 950-mb winds and potential vorticity at 1200 (a) and 1800 (b) UTC 30 July 2013.

August 2013 demonstrated once again that separation of the coastal jet is a large determinant in the propagation of a CTWR. Figure 39 is a snapshot of CTWR that took place in the hours of 19 August. Like the historical cases, the reversal was preceded by a very strong low-level coastal jet producing offshore flow and separation of the PV maximum from the coastline. A difference between this event in 2013 and the historical cases, evident not only in this case but in most of the "new" cases studied, is the sheer magnitude of PV present. Whereas the historical cases rarely displayed a PV maximum of even 60 PVU, the PV at 1800 UTC 19 August attained a magnitude of 100 PVU.

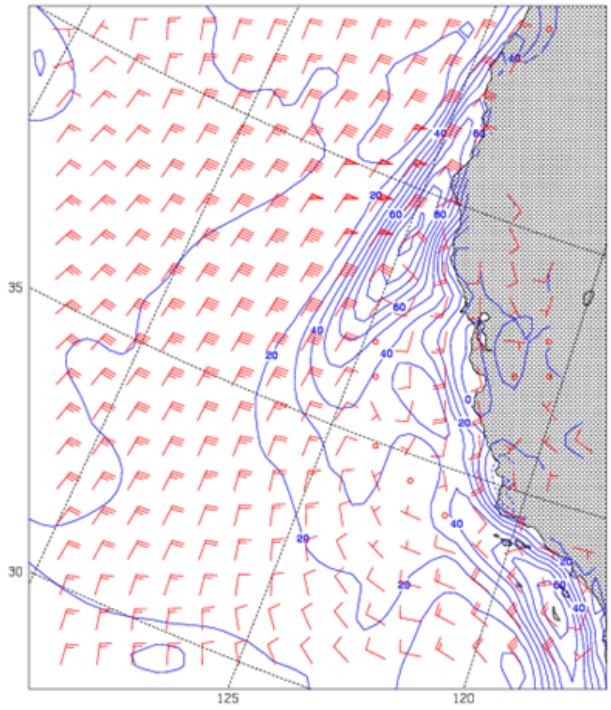


Figure 39. 950-mb winds and potential vorticity at 1800 UTC 19 August 2013.

In all, an analysis of the PV fields successfully captured the atmospheric viability of a CTWR. In the historical cases we determined that the separation of the coastal jet from the mountainous terrain of northern California was necessary to trigger southerly flow up the coast. In the "new" cases we were able to see a similar pattern emerge, though it became apparent that the establishment of an across-coast PV gradient was in fact more important than the separation of the jet itself. In multiple "new" cases, southerly winds were able to move north of Point Conception and into the Monterey Bay despite a lack of large westward displacement of the coastal jet. These events often had onshore rather than offshore flow in the vicinity just south of the PV maximum.

# V. CONCLUSIONS AND RECOMMENDATIONS

## A. CONCLUSIONS

At the onset of this study, we sought out to describe the evolution of a coastally trapped wind reversal through the analysis of its surrounding potential vorticity distribution. Specifically, the theory was to use the single parameter of PV to understand the synoptic evolution prior to the commencement of a CTWR. Toward that aim, the 950-mb PV distribution (or plumes) of six historical CTWR events was studied in search for common characteristics. Those characteristics were then applied to a set of suspected but unconfirmed wind reversals from 2012 and 2013 in order to determine their universal applicability.

The results from examining the potential vorticity of the historical CTWR events were relatively straightforward: the necessity for separation of the coastal jet from the terrain, the inconsequential nature of the orientation of the jet to the coastline, and tendency for the CTWR to develop an area of PV. Applying those results to the 14 suspected cases proved that we can characterize the synoptic environment using the single parameter of potential vorticity, although not in the manner originally expected. While it certainly held true that separation of the coastal jet from the coastline, specifically the associated PV maximum, was important, we found that establishment of an across-coast PV gradient was critical. This conclusion was borne out of examples from 2012/2013 where the coastal jet failed to separate from the coast yet a CTWR event still occurred as the PV associated with southerlies from Point Conception to Monterey pushed westward off the coast.

This conclusion about displacement and evolution of the PV maximum leads to another conclusion regarding the resolution of the CFSR dataset. While Mass and Bond (1996) used 383-km resolution data to piece together their climatology regarding the synoptic environment conducive for a CTWR, this thesis leaned on ~50-km resolution from the CFSR dataset to draw more subtle conclusions. For example, while Mass and Bond (1996) pointed to larger synoptic-scale features such as ridging into the Pacific

Northwest and troughing extending to the northwest from the valleys of central California, we were able to make conclusions about mesoscale features such as the small movement of the coastal jet or establishment of an across-coast PV gradient off the coast of Big Sur.

## B. RECOMMENDATIONS FOR FUTURE RESEARCH

Future research is needed to more thoroughly quantify the results for this study. We have shown that separation of the potential vorticity maximum, which derives from the interaction of the low-level coastal jet with mountainous terrain, from the coastline and establishment of an across-coast PV gradient is required for the northward propagation of a CTWR. However, can this distance be measured? Additionally, our work consistently relied on the subjective analysis of PV plumes and associated maxima. Is there a threshold of PVU that a PV maximum must attain before it generates a CTWR?

Work can also be undertaken to improve the temporal resolution of the data used. CFSR data was used for this study which was only available every six hours. As a CTWR is a mesoscale phenomenon that can travel relatively great distances in a short period of time, it is desirable to use a dataset with higher temporal resolution.

Finally, this study can be used as a stepping-stone to improve upon the Mass and Bond Climatology from 1996. In their work, Mass and Bond (1996) used 383-km data resolution for CTWRs from 1981–1991. That climatology then led to conclusions about what atmospheric parameters are required to enable a CTWR. One could build on that climatology by using the improved resolution of the CFSR data as well as adding information about the coastal jet and its required separation from the coast.

# LIST OF REFERENCES


Bond, N. A., C. F. Mass, and J. E. Overland, 1996: Coastally trapped wind reversals along the United States West Coast during the warm season. Part I: Climatology and temporal evolution. *Mon. Wea. Rev.*, **124**, 430–445.

Davis, C. A., and K. A. Emanuel, 1991: Potential vorticity diagnostics of cyclogenesis. *Mon. Wea. Rev.*, **119**, 1929–1953.

Dorman, C. E., 1985: Evidence of Kelvin waves in California's marine layer and related eddy generation. *Mon. Wea. Rev.*, **113**, 827–839.

Dorman, C. E., 1987: Possible role of gravity currents in Northern California's coastal summer wind reversals. *Journal of Geophysical Research*, **92**, 1497–1506.

Felsch, P., and W. Whitlatch, 1993: Stratus surge prediction along the central California coast. *Wea. Forecasting*, **8**, 204–213.

Mass, C. F., and M. D. Albright, 1987: Coastal southerlies and alongshore surges of the West Coast of North America: Evidence of mesoscale topographically trapped response to synoptic forcing. *Mon. Wea. Rev.*, **115**, 1707–1738.

Mass, C. F., and N. A. Bond, 1996: Coastally trapped wind reversals along the United States West Coast during the warm season. Part II: Synoptic evolution. *Mon. Wea. Rev.*, **124**, 446–461.

Nuss, W. A., 2007: Synoptic-scale structure and the character of coastally trapped wind reversals. *Mon. Wea. Rev.*, **135**, 60–81.

Nuss, W. A., J. M. Bane, W. T. Thompson, T. Holt, C. E. Dorman, F. M. Ralph, R. Rotunno, J. B. Klemp, W. C. Skamarock, R. M. Samelson, A. M. Rogerson, C. Reason, and P. Jackson, 2000: Coastally trapped wind reversals: Progress toward understanding. *Bull. Amer. Meteor. Soc.*, **81**, 719–744.

Parish, T. R., D. A. Rahn, and D. Leon, 2008: Aircraft observations of a coastally trapped wind reversal off the California coast. *Mon. Wea. Rev.*, **136**, 644–662.

Persson, P. O. G., P. J. Neiman, and M. F. Ralph, 1995: Topographically generated potential vorticity anomalies: A proposed mechanism for initiating orographically trapped disturbances. *Preprints, 7th AMS Conference on Mountain Meteorology,* 17–21 July 1995, Breckenridge, CO, 216–222.

Ralph, F. M., L. Armi, J. M. Bane, C. Dorman, W. D. Neff, P. J. Neiman, W. Nuss, and P. O. G. Persson, 1998: Observations and analysis of the 10–11 June 1994 coastally trapped disturbance. *Mon. Wea. Rev.*, **126**, 2435–2465.

Ralph, F. M., P. J. Neiman, J. M. Wilczak, P. O. G. Persson, J. M. Bane, M. L. Cancillo, and W. Nuss, 2000: Kelvin waves and internal bores in the marine boundary layer inversion and their relationship to coastally trapped wind reversals. *Mon. Wea. Rev.*, **128**, 283–300.

Reason, C. J. C., and D. G. Steyn, 1990: Coastally trapped disturbances in the lower atmostphere: Dynamic commonalities and geographic diversity. *Progress in Physical Geography*, **14**, 178–198.

Skamarock, W. C., R. Rotunno, and J. B. Klemp, 1999: Models of coastally trapped disturbances. *J. Atmos. Sci.*, **56**, 3349–4465.

# INITIAL DISTRIBUTION LIST

1. Defense Technical Information Center
   Ft. Belvoir, Virginia

2. Dudley Knox Library
   Naval Postgraduate School
   Monterey, California